

Ricci Flow and Bio–Reaction–Diffusion Systems

Vladimir G. Ivancevic*

Tijana T. Ivancevic†

Abstract

This paper proposes the Ricci–flow equation as a general geometric model for various reaction–diffusion systems (and related dissipative solitons) in mathematical biology. More precisely, we propose a hypothesis that any kind of reaction–diffusion processes in biology, chemistry and physics can be modelled by the combined geometric–diffusion system. In order to demonstrate the validity of this hypothesis, we review a number of popular reaction–diffusion systems and try to show that they are all subsumed by the presented geometric framework of the Ricci flow.

Keywords: Ricci flow, bio–reaction–diffusion, dissipative solitons and breathers

AMS: 53B20, 57N10, 92B99, 92C45

*Human Systems Integration, Land Operations Division, Defence Science & Technology Organisation, P.O. Box 1500, Edinburgh SA 5111, Australia (Vladimir.Ivancevic@dsto.defence.gov.au)

†School of Electrical and Information Engineering, University of South Australia, Mawson Lakes, S.A. 5095, Australia (Tijana.Ivancevic@unisa.edu.au)

Contents

1	Introduction	3
2	Bio–reaction–diffusion systems	6
2.1	1–component systems	8
2.1.1	Kolmogorov–Petrovsky–Piscounov equation	8
2.1.2	Swift–Hohenberg equation	9
2.1.3	Ginzburg–Landau equation	10
2.1.4	Neural field theory	11
2.2	2–component systems	12
2.2.1	Brusselator	13
2.2.2	2–component model of excitable media	14
2.2.3	Gierer–Meinhardt activator–inhibitor system	14
2.2.4	Fitzhugh–Nagumo activator–inhibitor system	15
2.2.5	2–component Belousov–Zhabotinsky reaction	16
2.3	3–component and multi–component systems	17
2.3.1	Oregonator	17
2.3.2	Multi–phase tumor growth equations	18
3	Dissipative evolution under the Ricci flow	20
3.1	Geometrization Conjecture	20
3.2	Reaction–diffusion–type evolution of curvatures and volumes	21
3.3	Dissipative solitons and Ricci breathers	27
3.3.1	Ricci breathers and Ricci solitons	27
3.4	Smoothing heat equation and Ricci entropy	28
3.5	Thermodynamic analogy	31
4	Appendix	32
4.1	Riemann and Ricci curvatures on a smooth n –manifold	32
4.2	n –component reactive temporal neurodynamics	34
4.2.1	Neurons as functions	34
4.2.2	Activation dynamics	35
4.2.3	Hopfield’s overlaps	37
4.2.4	Glauber vs. overlap dynamics	38
4.2.5	Generalized Hebbian learning dynamics	39
4.2.6	Lotka–Volterra–based associative net	41

1 Introduction

Parabolic *reaction–diffusion* systems are abundant in mathematical biology. They are mathematical models that describe how the concentration of one or more substances distributed in space changes under the influence of two processes: local chemical reactions in which the substances are converted into each other, and diffusion which causes the substances to spread out in space. More formally, they are expressed as semi–linear parabolic partial differential equations (PDEs, see e.g., [62]). The evolution of the state vector $\mathbf{u}(\mathbf{x}, t)$ describing the concentration of the different reagents is determined by anisotropic diffusion as well as local reactions:

$$\partial_t \mathbf{u} = \mathbf{D} \Delta \mathbf{u} + \mathbf{R}(\mathbf{u}), \quad (\partial_t = \partial/\partial t), \quad (1)$$

where each component of the state vector $\mathbf{u}(\mathbf{x}, t)$ represents the concentration of one substance, Δ is the standard Laplacian operator, \mathbf{D} is a symmetric positive–definite matrix of diffusion coefficients (which are proportional to the velocity of the diffusing particles) and $\mathbf{R}(\mathbf{u})$ accounts for all local reactions. The solutions of reaction–diffusion equations display a wide range of behaviors, including the formation of travelling waves and other self–organized patterns like *dissipative solitons* (DSs).

On the other hand, the *Ricci flow equation* (or, the parabolic Einstein equation), introduced by R. Hamilton in 1982 [16], is the nonlinear heat–like evolution equation¹

$$\partial_t g_{ij} = -2R_{ij}, \quad (2)$$

for a time–dependent Riemannian metric $g = g_{ij}(t)$ on a smooth real² n –manifold M with the Ricci curvature tensor R_{ij} .³ This equation roughly says that we can deform any metric on a 2–surface or n –manifold by the negative of its curvature; after *normalization*

¹The current hot topic in geometric topology is the Ricci flow, a Riemannian evolution machinery that recently allowed G. Perelman to prove the celebrated *Poincaré Conjecture*, a century–old mathematics problem (and one of the seven Millennium Prize Problems of the Clay Mathematics Institute) – and win him the 2006 Fields Medal (which he declined in a public controversy) [48]. The Poincaré Conjecture can roughly be put as a question: Is a closed 3–manifold M topologically a sphere if every closed curve in M can be shrunk continuously to a point? In other words, Poincaré conjectured: A simply-connected compact 3–manifold is diffeomorphic to the 3–sphere S^3 (see e.g., [71]).

²For the related Kähler–Ricci flow on complex manifolds, see e.g., [33, 34].

³This particular PDE (2) was chosen by Hamilton for much the same reason that A. Einstein introduced the Ricci tensor into his gravitation field equation,

$$R_{ij} - \frac{1}{2}g_{ij}R = 8\pi T_{ij},$$

where T_{ij} is the energy–momentum tensor. Einstein needed a symmetric 2–index tensor which arises naturally from the metric tensor g_{ij} and its first and second partial derivatives. The Ricci tensor R_{ij} is essentially the only possibility. In gravitation theory and cosmology, the Ricci tensor has the volume–decreasing effect (i.e., convergence of neighboring geodesics, see [27]).

(see Figure 1), the final state of such deformation will be a metric with constant curvature. The factor of 2 in (2) is more or less arbitrary, but the negative sign is essential to insure a kind of global *volume exponential decay*,⁴ since the Ricci flow equation (2) is a kind of nonlinear geometric generalization of the standard linear *heat equation*

$$\partial_t u = \Delta u. \quad (3)$$

Like the heat equation (3), the Ricci flow equation (2) is well behaved in forward time and acts as a kind of smoothing operator (but is usually impossible to solve in backward time). If some parts of a solid object are hot and others are cold, then, under the heat equation, heat will flow from hot to cold, so that the object gradually attains a uniform temperature. To some extent the Ricci flow behaves similarly, so that the Ricci curvature ‘tries’ to become more uniform [50], thus resembling a monotonic *entropy growth*,⁵ $\partial_t S \geq 0$, which is due to the positive definiteness of the metric $g_{ij} \geq 0$, and naturally implying the *arrow of time* [57, 34, 33].

In a suitable local coordinate system, the Ricci flow equation (2) has a nonlinear heat-type form, as follows. At any time t , we can choose local harmonic coordinates so that the coordinate functions are locally defined harmonic functions in the metric $g(t)$. Then the Ricci flow takes the general form (see e.g., [4])

$$\partial_t g_{ij} = \Delta_M g_{ij} + Q_{ij}(g, \partial g), \quad (4)$$

where Δ_M is the *Laplace–Beltrami operator* (5) and $Q = Q_{ij}(g, \partial g)$ is a lower-order term quadratic in g and its first order partial derivatives ∂g . From the analysis of nonlinear

⁴This complex geometric process is globally similar to a generic exponential decay ODE:

$$\dot{x} = -\lambda f(x),$$

for a positive function $f(x)$. We can get some insight into its solution from the simple exponential decay ODE,

$$\dot{x} = -\lambda x \quad \text{with the solution} \quad x(t) = x_0 e^{-\lambda t},$$

(where $x = x(t)$ is the observed quantity with its initial value x_0 and λ is a positive decay constant), as well as the corresponding n th order rate equation (where $n > 1$ is an integer),

$$\dot{x} = -\lambda x^n \quad \text{with the solution} \quad \frac{1}{x^{n-1}} = \frac{1}{x_0^{n-1}} + (n-1)\lambda t.$$

⁵Note that two different kinds of entropy functional have been introduced into the theory of the Ricci flow, both motivated by concepts of entropy in thermodynamics, statistical mechanics and information theory. One is Hamilton’s entropy, the other is Perelman’s entropy. While in Hamilton’s entropy, the scalar curvature R of the metric g_{ij} is viewed as the leading quantity of the system and plays the role of a probability density, in Perelman’s entropy the leading quantity describing the system is the metric g_{ij} itself. Hamilton established the monotonicity of his entropy along the volume-normalized Ricci flow on the 2-sphere S^2 [18]. Perelman established the monotonicity of his entropy along the Ricci flow in all dimensions [58].

heat PDEs, one obtains existence and uniqueness of forward-time solutions to the Ricci flow on some time interval, starting at any smooth initial metric g_0 .

The quadratic Ricci flow equation (4) is our geometric framework for general bio-reaction-diffusion systems, so that the spatio-temporal PDE (1) corresponds to the quadratic Ricci flow PDE

$$\begin{aligned} \partial_t \mathbf{u} &= \mathbf{D}\Delta \mathbf{u} + \mathbf{R}(\mathbf{u}) \\ \updownarrow & \quad \updownarrow \quad \quad \quad \updownarrow \\ \partial_t g_{ij} &= \Delta_M g_{ij} + Q_{ij}(g, \partial g) \end{aligned}$$

with:

- the metric $g = g_{ij}$ on an n -manifold M corresponding to the n -dimensional (or n -component, or n -phase) concentration $\mathbf{u}(\mathbf{x}, t)$;
- the Laplace-Beltrami differential operator Δ_M , as defined on C^2 -functions on an n -manifold M , with respect to the Riemannian metric g_{ij} , by

$$\Delta_M \equiv \frac{1}{\sqrt{\det(g)}} \frac{\partial}{\partial x^i} \left(\sqrt{\det(g)} g^{ij} \frac{\partial}{\partial x^j} \right) \quad (5)$$

– corresponding to the n -dimensional bio-diffusion term $\mathbf{D}\Delta \mathbf{u}$; and

- the quadratic n -dimensional Ricci-term, $Q = Q_{ij}(g, \partial g)$, corresponding to the n -dimensional bio-reaction term, $\mathbf{R}(\mathbf{u})$.

As a simple example of the Ricci flow equations (2)–(4), consider a round spherical boundary S^2 of the 3-ball radius r . The metric tensor on S^2 takes the form

$$g_{ij} = r^2 \hat{g}_{ij},$$

where \hat{g}_{ij} is the metric for a unit sphere, while the Ricci tensor

$$R_{ij} = (n - 1) \hat{g}_{ij}$$

is independent of r . The Ricci flow equation on S^2 reduces to

$$\dot{r}^2 = -2(n - 1), \quad \text{with the solution} \quad r^2(t) = r^2(0) - 2(n - 1)t.$$

Thus the boundary sphere S^2 collapses to a point in finite time (see [50]).

More generally, the following geometrization conjecture [67] holds for any 3-manifold M : Suppose that we start with a compact initial 3-manifold M_0 whose Ricci tensor R_{ij} is everywhere positive definite. Then, as M_0 shrinks to a point under the Ricci flow (2), it becomes rounder and rounder. If we rescale the metric g_{ij} on M_0 so that the volume

of M_0 remains constant, then M_0 converges towards another compact 3-manifold M_1 of constant positive curvature (see [16]).

In case of even more general 3-manifolds (outside the class of positive Ricci curvature metrics), the situation is much more complicated, as various singularities may arise. One way in which singularities may arise during the Ricci flow is that a spherical boundary $S^2 = \partial M$ of an 3-manifold M may collapse to a point in finite time. Such collapses can be eliminated by performing a kind of ‘geometric surgery’ on the 3-manifold M , that is a sophisticated sequence of cutting and pasting without accumulation of time errors⁶ (see [59]). After a finite number of such surgeries, each component either: (i) converges towards a 3-manifold of constant positive Ricci curvature which shrinks to a point in finite time, or possibly (ii) converges towards an $S^2 \times S^1$ which shrinks to a circle S^1 in finite time, or (iii) admits a ‘thin-thick’ decomposition of [67]. Therefore, one can choose the surgery parameters so that there is a well defined Ricci flow with surgery, that exists for all time [59].

In this paper we use the evolving n -dimensional geometric machinery of the volume-decaying and entropy-growing Ricci flow $g(t)$, given by equations (2)–(4), for modelling various biological reaction-diffusion systems and dissipative solitons, defined by special cases of the general spatio-temporal model (1).

2 Bio-reaction-diffusion systems

In case of ideal mixtures, the driving force for the general diffusion $\mathbf{D}\Delta\mathbf{u}$ (1) is the concentration gradient $-\nabla\mathbf{u}$, or the gradient of the chemical potential $-\nabla u_i$ of each species u_i , ($i = 1, \dots, n$), giving the *diffusion flux* by the First Fick’s law,

$$J = -\mathbf{D}\nabla\mathbf{u}. \quad (6)$$

Assuming the diffusion coefficients \mathbf{D} to be a constant, the Second Fick’s law gives the linear parabolic heat equation,

$$\partial_t\mathbf{u} = \mathbf{D}\Delta\mathbf{u}, \quad (7)$$

while, in case of variable diffusion coefficients \mathbf{D} , we get (slightly) more general parabolic *diffusion equation*,

$$\partial_t\mathbf{u} = \nabla \cdot (\mathbf{D}\nabla\mathbf{u}), \quad (8)$$

⁶Hamilton’s idea was to perform surgery to cut off the singularities and continue his flow after the surgery. If the flow develops singularities again, one repeats the process of performing surgery and continuing the flow. If one can prove there are only a finite number of surgeries in any finite time interval, and if the long-time behavior of solutions of the Ricci flow (2) with surgery is well understood, then one would be able to recognize the topological structure of the initial manifold. Thus Hamilton’s program, when carried out successfully, would lead to a proof of the Poincaré Conjecture and Thurston’s Geometrization Conjecture [71].

which is still analogous to the ‘linear’ part of the quadratic Ricci flow equation (4),

$$\partial_t g_{ij} = \Delta_M g_{ij},$$

due to general ‘diffusion properties’ of the Laplace–Beltrami operator Δ_M .

The n –dimensional diffusion coefficient $\mathbf{D} = \mathbf{D}(T)$ at different temperatures T can be approximated by the Arrhenius exponential–decay relation,

$$\mathbf{D}(t) = \mathbf{D}_0 e^{-\frac{E_A}{rT}},$$

where \mathbf{D}_0 is the maximum possible diffusion coefficient (at infinite temperature T), E_A is the activation energy for diffusion (i.e., the energy that must be overcome in order for a chemical reaction to occur) and r is the gas constant.

Using the First Fick’s first law (6), the diffusion equation (8) can be derived in a straightforward way from the *continuity equation*, which states that a change in density in any part of the system is due to inflow and outflow of material into and out of that part of the system (effectively, no material is created or destroyed),

$$\partial_t \mathbf{u} + \nabla \cdot \mathbf{j} = 0,$$

where \mathbf{j} is the flux of the diffusing material.

The most important special case of (7) is at a steady state, when the concentrations \mathbf{u} do not change in time, giving the *Laplace’s equation*,

$$\Delta \mathbf{u} = 0, \quad \text{or} \quad \Delta u_i = 0, \quad (9)$$

for harmonic functions $\mathbf{u} = \{u_i\}$.

The stochastic version of the deterministic heat equation (7), connected with the study of Brownian motion,⁷ is the *Fokker–Planck equation* (see e.g., [37]),

$$\partial_t f = -\partial_{x^i} [D_i^1(x^i) f] + \partial_{x^i x^j} [D_{ij}^2(x^i) f], \quad (10)$$

($\partial_{x^i} = \frac{\partial}{\partial x_i}$, $\partial_{x^i x^j} = \frac{\partial^2}{\partial x_i \partial x_j}$), where where D_i^1 is the drift vector and D_{ij}^2 the diffusion tensor (which results from the presence of the stochastic force). The Fokker–Planck equation (10) is used for computing the probability densities of stochastic differential equations.⁸

⁷Brownian motion is the random movement of particles suspended in a liquid or gas or the mathematical model used to describe such random movements, often called a particle theory. The infinitesimal generator (and hence characteristic operator) of a Brownian motion on \mathbb{R}^n is $\frac{1}{2}\Delta$, where Δ is the Laplacian on \mathbb{R}^n . More generally, a Brownian motion on an n –manifold M is given by one-half of the Laplace–Beltrami operator Δ_M (5).

⁸Consider the Itô stochastic differential equation,

$$d\mathbf{X}_t = \boldsymbol{\mu}(\mathbf{X}_t, t) dt + \boldsymbol{\sigma}(\mathbf{X}_t, t) d\mathbf{W}_t,$$

Also, notice that the real-valued heat equation (7) is formally similar to the complex-valued *Schrödinger equation* (see e.g., [38]),

$$\partial_t \psi = \frac{i\hbar}{2m} \Delta \psi, \quad (11)$$

where $\psi = \psi(\mathbf{x}, t)$ is the wave-function of the particle, $i = \sqrt{-1}$, and \hbar is Planck's constant divided by 2π .

In the remainder of this section, we will review a number of particular bio-reaction-diffusion systems, which can all be subsumed by the quadratic Ricci flow model (4).

2.1 1-component systems

2.1.1 Kolmogorov-Petrovsky-Piscounov equation

The simplest bio-reaction-diffusion PDE concerning the concentration $u = u(x, t)$ of a single substance in one spatial dimension,

$$\partial_t u = D \partial_x^2 u + R(u), \quad (12)$$

is also referred to as the Kolmogorov-Petrovsky-Piscounov (KPP) equation. If the reaction term vanishes, then the equation represents a pure diffusion process described by the heat equation. In particular, the choice

$$R(u) = u(1 - u)$$

yields *Fisher's equation* that was originally used to describe the spreading of biological populations.⁹

where $\mathbf{X}_t \in \mathbb{R}^n$ is the state of an n -dimensional stochastic system at time t and $\mathbf{W}_t \in \mathbb{R}^m$ is the standard m D Wiener process. If the initial distribution is $\mathbf{X}_0 \sim f(\mathbf{x}, 0)$, then the probability density of the state is given by the Fokker-Planck equation (10) with the drift and diffusion terms,

$$D_i^1(\mathbf{x}, t) = \mu_i(\mathbf{x}, t) \quad \text{and} \quad D_{ij}^2(\mathbf{x}, t) = \frac{1}{2} \sum_k \sigma_{ik}(\mathbf{x}, t) \sigma_{kj}^\top(\mathbf{x}, t).$$

⁹In addition, the effects of convection and quenched spatial disorder on the evolution of a population density are described by a generalization of the Fisher/KPP equation given by [55]

$$\partial_t u = D \nabla^2 u + U u - q u^2,$$

where $u = u(\mathbf{x}, t)$ represents the population density, D is a spatially homogenous diffusion constant, $U = U(\mathbf{x})$ is a spatially inhomogeneous growth term, and $q = b \ell_0^d$ is a competition term (b is a competition rate and ℓ_0 is the microscopic length scale at which two particles will compete with one another). One simple form of inhomogeneity considered in these works is a 'square well' potential $U(\mathbf{x})$ which consists of a uniform space with negative growth rate (termed the 'desert'), in which a single region of positive growth rate (an 'oasis') is placed. This model has proven to be applicable to experiments with bacteria populations in adverse environments [52].

The one-component KPP equation (12) can also be written in the variational (gradient) form

$$\partial_t u = -\frac{\delta F}{\delta u}, \quad (13)$$

and therefore describes a permanent decrease (a kind of exponential decay) of the system's *free energy* functional

$$F = \int_{-\infty}^{\infty} \left[\frac{D}{2} (\partial_x u)^2 + V(u) \right] dx,$$

where $V(u)$ is the potential such that

$$R(u) = -\frac{dV(u)}{du}. \quad (14)$$

2.1.2 Swift–Hohenberg equation

The Swift–Hohenberg (SH) equation, noted for its pattern-forming behavior, is the decaying reaction–diffusion PDE,

$$\partial_t u = -(1 + \Delta)u + R(u), \quad (15)$$

given by the variational (gradient) equation (13) with the free energy functional

$$F = \int_{\Omega} \left[V(u) + \frac{1}{2} ((1 + \Delta)u)^2 \right] dx dy,$$

where $R(u)$ is given by (14), while Ω is a 2-dimensional region in which (bio)chemical pattern formation occurs.

The time derivative of the free energy F is given by

$$\partial_t F = \int_{\Omega} \left[\frac{dV(u)}{du} + (1 + \Delta)u \right] \partial_t u \, dx dy,$$

and, since the expression in square brackets is equal to the negative right-hand side of (15), we have

$$\dot{F} = - \int_{\Omega} (\partial_t u)^2 \, dx dy \leq 0.$$

Therefore, the free energy F is the *Lyapunov functional* that may only decrease as it evolves along its trajectory in some phase space. If F has no minima, then when the horizontal scale of the liquid container is large compared to the instability wavelength, a

propagating front will be observed (e.g., in chemically reacting flames). In this case, F will decrease continuously until the front approaches the boundary of the medium. An alternative possibility is realized when F has one or several minima, each corresponding to a local equilibrium state in time. In this case the so-called multi-stability is possible. Therefore, the limit behavior of gradient systems of the form of (14) is characterized by either a steady attractor or propagating fronts [63].

2.1.3 Ginzburg–Landau equation

One of the most popular models in the pattern-formation theory is the complex Ginzburg–Landau equation (see e.g., [63]),

$$\partial_t A = \varepsilon A + (1 + i\alpha)\Delta A - (1 + i\beta)|A|^2 A, \quad (16)$$

where A is the complex wave amplitude, $i = \sqrt{-1}$, ε is the super-criticality parameter, while α and β measure linear and nonlinear dispersion (the dependence of the frequency of the waves on the wave-number), respectively. The equation (16) describes a vast array of phenomena including nonlinear waves, second-order phase transitions, Rayleigh–Bénard convection and superconductivity. The equation describes the evolution of amplitudes of unstable modes for any process exhibiting a Hopf bifurcation, for which a continuous spectrum of unstable wave-numbers is taken into account. It can be viewed as a highly general normal form for a large class of bifurcations and nonlinear wave phenomena in spatially extended systems.¹⁰

In particular, if we put $\alpha = \beta = 0$ in (16), we get the real, or dissipative, Ginzburg–Landau equation,

$$\partial_t A = \varepsilon A + \Delta A - |A|^2 A, \quad (18)$$

¹⁰The extension of the complex Ginzburg–Landau equation (16), which describes strongly resonant multi-frequency forcing of the form

$$F = f_1 e^{i\omega\bar{t}} + f_2 e^{2i\omega\bar{t}} + f_3 e^{3i\omega\bar{t}} + c.c.$$

was recently proposed in [9] by considering the analogous center-manifold reduction of the extended dynamical system in which the forcing amplitudes f_1 , f_2 , and f_3 are considered as dynamical variables that vary on the slow time scale t . Under time translations $T_\tau : A \rightarrow Ae^{i\omega\tau}$, they transform as $f_1 \rightarrow f_1 e^{i\omega\tau}$, $f_2 \rightarrow f_2 e^{2i\omega\tau}$, $f_3 \rightarrow f_3 e^{3i\omega\tau}$. To cubic order in A the most general equation that is equivariant under T_τ is then given by

$$\partial_t A = a_1 + a_2 A + a_3 \Delta A + a_4 |A|^2 + a_5 \bar{A} + a_6 \bar{A}^2, \quad (17)$$

where $a_1 = b_{11}f_1 + b_{12}\bar{f}_2f_3$, $a_2 = b_{21} + b_{22}|f_3|^2$, $a_5 = b_{51}f_2$, $a_6 = b_{61}f_3$. The forcing terms f_j satisfy decoupled evolution equations on their own. In the simplest case this evolution expresses a de-tuning ν_j of the forcing f_j from the respective resonance and the f_j satisfy

$$\dot{f}_j = i\nu_j f_j, \quad (j = 1 \dots 3).$$

In general, the de-tuning introduces time dependence into (17).

which is a gradient equation: $\partial_t A = -\delta F/\delta A$, with the free energy functional

$$F = - \int_{\Omega} \left[\varepsilon |A|^2 - \frac{1}{2} |A|^4 + (\nabla A)^2 \right] dx dy.$$

Using the fact that

$$\dot{F} = - \int_{\Omega} |\partial_t A|^2 dx dy \leq 0,$$

solutions of (18) at $t \rightarrow \infty$ are either stationary field-distributions satisfying, for $\varepsilon = 1$, the equation

$$\Delta A + A - |A|^2 A = 0, \tag{19}$$

of fronts whose propagation is accompanied by a decrease of the functional F . The functional must reach its minimum at stable stationary solutions of (19).

2.1.4 Neural field theory

The dynamical system from which the temporal evolution of neural activation fields (see Appendix) is generated is constrained by the postulate that localized peaks of activation are stable objects, or formally, *fixed-point attractors*. Such a field dynamics has the generic form [65]

$$\tau \partial_t u = -u + \text{resting level} + \text{input} + \text{interaction}, \tag{20}$$

where $u = u(x, t)$ is the activation field defined over the metric dimension x and time t . The first three terms define an input driven regime, in which attractor solutions have the form

$$u(x, t) = \text{resting level} + \text{input}.$$

The *rate of relaxation* is determined by the time scale parameter τ . The interaction stabilizes localized peaks of activation against decay by local excitatory interaction and against diffusion by global inhibitory interaction. In Amari's formulation [3] the conceptual model (20) is specified as a *continuous model for neural activity in cortical structures*,

$$\tau \partial_t u(x, t) = -u(x, t) + h + S(x, t) + \int dx' w(x - x') \sigma(u(x', t)), \tag{21}$$

where $h < 0$ is a constant resting level, $S(x, t)$ is spatially and temporally variable input function, $w(x)$ is an interaction kernel and $\sigma(u)$ is a sigmoidal nonlinear threshold function. The interaction term collects input from all those field sites x' at which activation is sufficiently large. The interaction kernel determines if inputs from those sites are positive, driving up activation (excitatory), or negative, driving down activation (inhibitory). Excitatory input from nearby location and inhibitory input from all field locations generically

stabilizes localized peaks of activation. For this class of dynamics, detailed analytical results provide a framework for the inverse dynamics task facing the modeler, determining a dynamical system that has the appropriate attractor solutions [32, 39].¹¹

2.2 2–component systems

Two–component systems allow for a much larger range of possible phenomena than their one–component counterparts. An important idea that was first proposed by A. Turing is that a state that is stable in the local system should become unstable in the presence of diffusion [68]. This idea seems counter–intuitive at first glance as diffusion is commonly associated with a stabilizing effect. However, the linear stability analysis shows that when

¹¹Recently, a *neural attractor dynamics* (NAD) was designed (see [65]) based on a discretization for single neurons of Amari’s neural field equation (21). The so–called *discrete Amari equation* describes the temporal evolution of the activity of all single neurons considering positive and negative contributions from external input and internal neural interactions. Since only activated neurons can have an impact on other neurons, the neural attractor dynamics is nonlinear, and effects of bi–stability and hysteresis can be used for low–level memory and neural competition. The NAD describes the temporal rate of change of the dynamical variable u_i of neural activity for all behavioral neurons i . It is formulated as the following differential equation:

$$\tau \dot{u}_i = -u_i + h + s_i^{\text{beh}} + c_{\text{mot}} \cdot \sigma(m_i) + \alpha_{\text{selfexc},i}^{\text{beh}} + \alpha_{\text{exc},i}^{\text{beh}} - \alpha_{\text{inh},i}^{\text{beh}}, \quad (22)$$

where the system parameters have the following meaning:

- τ , the constant relaxation rate, i.e., the time scale on which the dynamics reacts to changes;
- h , the constant negative resting level of neural activation;
- $\sigma(\cdot)$, a sigmoidal function, which maps the value of neural activity onto $[0, 1]$, given by $\sigma(u) = \frac{1}{1+e^{-\beta u}}$, where β ($=100$) parameterizes the slope of the resulting function;
- s_i^{beh} , the adequate stimulus provided by sensory input of a certain duration;
- u_i , activity of behavioral neuron i , i.e., activity of behavior i ;
- c_{mot} , a constant for weighting the motivational contribution, $c_{\text{mot}} < |h|$;
- $\alpha_{\text{selfexc},i}^{\text{beh}}$ excitatory contribution of neuron i ’s own activity u_i ;
- $\alpha_{\text{exc},i}^{\text{beh}}$, all excitatory contribution of active neurons connected to neuron i ;
- $\alpha_{\text{inh},i}^{\text{beh}}$, all inhibitory contribution of active neurons connected to neuron i ;
- m_i , activity of motivational neuron i , i.e., motivation of behavior i is in [65] defined by the following NAD–equation, similar to (22):

$$\tau \dot{m}_i = -m_i + h + s_i^{\text{mot}} + \alpha_{\text{selfexc},i}^{\text{mot}} + \alpha_{\text{exc},i}^{\text{mot}} - \alpha_{\text{inh},i}^{\text{mot}},$$

where

- $\alpha_{\text{selfexc},i}^{\text{mot}}$, excitatory contribution of neuron i ’s own motivation m_i ;
- $\alpha_{\text{exc},i}^{\text{mot}}$, all excitatory contribution of motivation neurons connected to neuron i ;
- $\alpha_{\text{inh},i}^{\text{mot}}$, all inhibitory contribution of motivation neurons connected to neuron i .

In this framework, a nonlinear neural dynamical and control system generates the temporal evolution of behavioral variables, such that desired behaviors are fixed–point attractor solutions while un–desired behaviors are repellers.

This kind of *attractor & repeller dynamics* [32] provides the basis for understanding *cognition*, both natural and artificial [39, 35, 36].

linearizing the general two-component system

$$\begin{pmatrix} \partial_t u \\ \partial_t v \end{pmatrix} = \begin{pmatrix} D_u & 0 \\ 0 & D_v \end{pmatrix} \begin{pmatrix} \partial_{xx} u \\ \partial_{xx} v \end{pmatrix} + \begin{pmatrix} F(u, v) \\ G(u, v) \end{pmatrix}$$

and perturbing the system against plane waves

$$\tilde{\mathbf{u}}_{\mathbf{k}}(\mathbf{x}, t) = \begin{pmatrix} \tilde{u}(t) \\ \tilde{v}(t) \end{pmatrix} e^{i\mathbf{k}\cdot\mathbf{x}}$$

close to a stationary homogeneous solution one finds [36]

$$\begin{pmatrix} \partial_t \tilde{u}_{\mathbf{k}}(t) \\ \partial_t \tilde{v}_{\mathbf{k}}(t) \end{pmatrix} = -k^2 \begin{pmatrix} D_u \tilde{u}_{\mathbf{k}}(t) \\ D_v \tilde{v}_{\mathbf{k}}(t) \end{pmatrix} + \mathbf{R}' \begin{pmatrix} \tilde{u}_{\mathbf{k}}(t) \\ \tilde{v}_{\mathbf{k}}(t) \end{pmatrix}.$$

Turing's idea can only be realized in four equivalence classes of systems characterized by the signs of the Jacobian \mathbf{R}' of the reaction function. In particular, if a finite wave vector \mathbf{k} is supposed to be the most unstable one, the Jacobian must have the signs

$$\begin{pmatrix} + & - \\ + & - \end{pmatrix}, \quad \begin{pmatrix} + & + \\ - & - \end{pmatrix}, \quad \begin{pmatrix} - & + \\ - & + \end{pmatrix}, \quad \begin{pmatrix} - & - \\ + & + \end{pmatrix}.$$

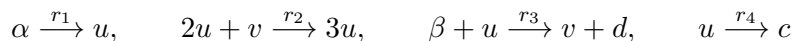
This class of systems is named activator–inhibitor system after its first representative: close to the ground state, one component stimulates the production of both components while the other one inhibits their growth. Its most prominent representative is the FitzHugh–Nagumo equation (25).

2.2.1 Brusselator

Classical model of an autocatalytic chemical reaction is Prigogine's Brusselator (see e.g., [61])

$$\partial_t u = D_u^2 \Delta u + \alpha + u^2 v - (1 + \beta)u, \quad \partial_t v = D_v^2 \Delta v - u^2 v + \beta u, \quad (23)$$

which describe the spatio-temporal evolution of the intermediate components u and v , with diffusion coefficients D_u and D_v , while reactions



describe the concentration of the original substances α and β , for which the final products c and d are constant when all four reaction rates r_i equal unity.

A discretized (temporal only) version of the Brusselator PDE (23) reads

$$\dot{u} = \alpha + u^2 v - (1 + \beta)u, \quad \dot{v} = \beta u - u^2 v.$$

The Brusselator displays oscillatory behavior in the species u and v when reverse reactions are neglected and the concentrations of α and β are kept constant.

2.2.2 2–component model of excitable media

Turbulence of scroll waves is a kind of spatio–temporal chaos that exists in 3–dimensional excitable media. Cardiac tissue and the Belousov–Zhabotinsky reaction are examples of such media. In cardiac tissue, chaotic behavior is believed to underlie fibrillation which, without intervention, precedes cardiac death. Fast computer–simulation of waves in excitable media have been often performed using the 2–component Barkley model of excitable media [5],

$$\partial_t u = \frac{1}{\epsilon} u(1-u) \left(u - \frac{v+b(t)}{a} \right) + \nabla^2 u + h(t), \quad \partial_t v = u - v, \quad (24)$$

where ϵ is a small parameter $\epsilon \ll 1$ characterising mutual time scales of the fast u and slow v variables, and a and b specify the kinetic properties of the system. Parameter b determines the excitation threshold and thus controls the excitability of the medium. The term $h(t)$ represents an ‘extra transmembrane current’.

Suppression of the turbulence using stimulation of two different types, ‘modulation of excitability’ and ‘extra transmembrane current’ was performed in [53], using the Barkley model (24). With cardiac defibrillation in mind, the authors used a single pulse as well as repetitive extra current with both constant and feedback controlled frequency. They show that turbulence can be terminated using either a resonant modulation of excitability or a resonant extra current. The turbulence is terminated with much higher probability using a resonant frequency perturbation than a non-resonant one. Suppression of the turbulence using a resonant frequency is up to fifty times faster than using a non-resonant frequency, in both the modulation of excitability and the extra current modes. They also demonstrate that resonant perturbation requires strength one order of magnitude lower than that of a single pulse, which is currently used in clinical practice to terminate cardiac fibrillation.

2.2.3 Gierer–Meinhardt activator–inhibitor system

Spontaneous pattern formation in initially almost homogeneous systems is common in both organic and inorganic systems. The Gierer–Meinhardt model [14] is a reaction–diffusion system of the activator–inhibitor type that appears to account for many important types of pattern formation and morphogenesis observed in biology, chemistry and physics. The model describes the concentration of a short–range autocatalytic substance, the activator, that regulates the production of its long–range antagonist, the inhibitor. It is given as a 2–component nonlinear PDE system,

$$\partial_t a = -\mu_a a + \rho a^2/h + D_a \partial_{x^2} a + \rho_a, \quad \partial_t h = -\mu_h h + \rho a^2 + D_h \partial_{x^2} h + \rho_h,$$

where a is a short–range autocatalytic substance, i.e., *activator*, and h is its long–range antagonist, i.e., *inhibitor*. $\partial_t a$ and $\partial_t h$ describe respectively the changes of activator and

inhibitor concentrations per second, μ_a and μ_h are the corresponding decay rates, while D_a and D_h are the corresponding diffusion coefficients. ρ is a positive constant. ρ_a is a small activator-independent production rate of the activator and is required to initiate the activator autocatalysis at very low activator concentration, e.g., in the case of regeneration. A low baseline production of the inhibitor, ρ_h , leads to a stable non-patterned steady state; the system can be asleep until an external trigger occurs by an elevation of the activator concentration above a threshold [49].

2.2.4 Fitzhugh–Nagumo activator–inhibitor system

An important example of bio-reaction-diffusion systems, frequently used in neurodynamics, is the 2-component Fitzhugh–Nagumo activator–inhibitor system [12, 54] (see also [30, 35])

$$\tau_u \partial_t u = D_u^2 \Delta u + f(u) - \sigma v, \quad \tau_v \partial_t v = D_v^2 \Delta v + u - v, \quad (25)$$

with $f(u) = \lambda u - u^3 - \kappa$, which describes how an action potential travels through a nerve, D_u and D_v are diffusion coefficients, τ_u and τ_v are time characteristics, while κ, σ and λ are positive constants. In matrix form, system (25) reads

$$\begin{pmatrix} \tau_u \partial_t u \\ \tau_v \partial_t v \end{pmatrix} = \begin{pmatrix} D_u^2 & 0 \\ 0 & D_v^2 \end{pmatrix} \begin{pmatrix} \Delta u \\ \Delta v \end{pmatrix} + \begin{pmatrix} \lambda u - u^3 - \kappa - \sigma v \\ u - v \end{pmatrix}.$$

When an activator–inhibitor system undergoes a change of parameters, one may pass from conditions under which a homogeneous ground state is stable to conditions under which it is linearly unstable. The corresponding bifurcation may be either a *Hopf bifurcation* to a globally oscillating homogeneous state with a dominant wave number $k = 0$ or a *Turing bifurcation* to a globally patterned state with a dominant finite wave number. The latter in two spatial dimensions typically leads to stripe or hexagonal patterns.

In particular, for the Fitzhugh–Nagumo system (25), the neutral stability curves marking the boundary of the linearly stable region for the Turing and Hopf bifurcation are given by

$$\begin{aligned} q_n^H(k) &: \frac{1}{\tau} + (d_u^2 + \frac{1}{\tau} d_v^2) k^2 = f'(u_h), \\ q_n^T(k) &: \frac{\kappa_3}{1 + d_v^2 k^2} + d_u^2 k^2 = f'(u_h). \end{aligned}$$

If the bifurcation is subcritical, often localized structures (i.e., dissipative solitons) can be observed in the hysteretic region where the pattern coexists with the ground state. Other frequently encountered structures comprise pulse trains, spiral waves and target patterns.

The reduced (temporal) non-dimensional Fitzhugh–Nagumo equations read:

$$\dot{v} = v(a - v)(v - 1) - w + I_a, \quad (26)$$

$$\dot{w} = bv - \gamma w, \quad (27)$$

where $0 < a < 1$ is essentially the threshold value, b and γ are positive constants and I_a is the applied current. The drift field for this model is given by

$$u_1(v, w) = v(a - v)(v - 1) - w, \quad u_2(v, w) = bv - \gamma w.$$

As can be seen from (27) the null cline of the deterministic dynamics of this equations is the line $v = \frac{\gamma}{b}w$. By substitution on the r.h.s of equation (26) we find the following equation for steady states: $v(a - v)(v - 1) - \frac{b}{\gamma}v = 0$.

When this system is in a noisy environment, in the limit of weak noise, we can approximate the dynamics of the fluctuations by the *Langevin equation* [30, 37]

$$\dot{v} = v(a - v)(v - 1) - \frac{b}{\gamma}v + \xi(t),$$

that is, the fluctuations run along the line $v = \frac{\gamma}{b}w$.

In particular, parameters in the *FitzHugh–Nagumo neuron* model [39, 36]

$$\dot{v} = a + bv + cv^2 + dv^3 - u, \quad \dot{u} = \varepsilon(ev - u),$$

can be tuned so that the model describes spiking dynamics of many resonator neurons (for details on neurons, see Appendix). Since one needs to simulate the shape of each spike, the time step in the model must be relatively small, e.g., $\tau = 0.25 \text{ ms}$. Since the model is a 2–dimensional system of ODEs, without a reset, it cannot exhibit autonomous chaotic dynamics or bursting. Adding noise to this, or some other 2–dimensional models, allows for stochastic bursting.

2.2.5 2–component Belousov–Zhabotinsky reaction

Classical Belousov–Zhabotinsky (BZ) reaction is a family of oscillating chemical reactions. During these reactions, transition–metal ions catalyze oxidation of various, usually organic, reductants by bromic acid in acidic water solution. Most BZ reactions are homogeneous. The BZ reaction makes it possible to observe development of complex patterns in time and space by naked eye on a very convenient human time scale of dozens of seconds and space scale of several millimeters. The BZ reaction can generate up to several thousand oscillatory cycles in a closed system, which permits studying chemical waves and patterns without constant replenishment of reactants [73].

Consider the water–in–oil micro–emulsion BZ reaction [41, 40]

$$\begin{aligned} \partial_t v &= D_v \Delta v + \frac{1}{\varepsilon_0} [f_0 z + i_0 (1 - mz)] \frac{v - q_0}{v + q_0} + \frac{1}{\varepsilon_0} \left[\frac{1 - mz}{1 - mz + \varepsilon_1} \right] v - v^2, \\ \partial_t z &= D_z \Delta z - z + v \left[\frac{1 - mz}{1 - mz + \varepsilon_1} \right], \end{aligned} \tag{28}$$

where v, z are dimensionless concentrations of activator HBrO_2 and oxidized catalyst $[\text{Ru}(\text{bpy})_3]^{3+}$ respectively; D_v and D_z are dimensionless diffusion coefficients of activator and catalyst; $f, \varepsilon_0, \varepsilon_1$ and q are parameters of the standard Tyson model [69]; i_0 represents the photoinduced production of inhibitor, and m represents the strength of oxidized state of the catalyst with $0 < mz < 1$. This reaction was shown experimentally and numerically to admit localized spot patterns that persist for long time [41, 40].

We can rescale the variables in (28) as [43]

$$z = 1/m - m^{-3/2}w\varepsilon_1, \quad v = m^{-1/2}\hat{v}, \quad t = \varepsilon_0 m^{1/2}\hat{t}.$$

In the new variables, after dropping the hats, we obtain the non-dimensional 2-component BZ reaction

$$\partial_t v = \varepsilon^2 \Delta v + f(v, w), \quad \tau \partial_t w = D \Delta w + g(v, w),$$

where

$$f(v, z) = -[f_0 + f_1 w] \frac{v - q}{v + q} + \left[\frac{w}{1 + \alpha w} \right] v - v^2, \quad g(v, w) = 1 - \left[\frac{w}{1 + \alpha w} \right] v,$$

with the non-dimensional constants given by

$$\begin{aligned} \alpha &= m^{-1/2}, & f_1 &= \varepsilon_1 m^{1/2} \left(i_0 - \frac{f_0}{m} \right), & q &= q_0 m^{1/2}, \\ \varepsilon^2 &= \varepsilon_0 D_v m^{1/2}, & D &= D_z \varepsilon_1 m^{-1/2}, & \tau &= \frac{1}{m} \frac{\varepsilon_1}{\varepsilon_0}. \end{aligned}$$

2.3 3-component and multi-component systems

2.3.1 Oregonator

The Oregonator model is based on the so-called FKN-mechanism [11], which provided the first successful explanation of the chemical oscillations that occur in the experimental Belousov-Zhabotinsky reaction. It is composed of five coupled elementary chemical stoichiometries. During the last two decades, the Oregonator model has been modified in many ways by inclusion of additional chemical reaction steps or by changing the rate constants. If we denote the concentration of the species S by [S], then we define: $A = [\text{BrO}_3^-]$, $H = [\text{H}^+]$, $X = [\text{HBrO}_2]$, $Y = [\text{Br}^-]$, $Z = [\text{Ce}^{4+}]$. The original Oregonator model was described by the following three coupled nonlinear PDEs,

$$\begin{aligned} \partial_t X &= k_1 A H^2 Y - k_2 H X Y - 2k_3 X^2 + k_4 A H X + D_X \nabla_{\mathbf{r}}^2 X, \\ \partial_t Y &= -k_1 A H^2 Y - k_2 H X Y + k_5 f Z + D_Y \nabla_{\mathbf{r}}^2 Y, \\ \partial_t Z &= 2k_4 A H X - k_5 Z + D_Z \nabla_{\mathbf{r}}^2 Z, \end{aligned} \tag{29}$$

where f is a stoichiometric factor [56], $k_i (i = 1, \dots, 5)$ are rate constants, while D_X , D_Y , and D_Z are the diffusion constants of the species HBrO_2 , Br^- , and Ce^{4+} respectively (for dilute solutions, the diffusion matrix is diagonal). For a thorough discussion of the chemistry on which the Oregonator is based, the reader is referred to [69].

The Oregonator temporal mass–action dynamics is a well–stirred, homogeneous system of ODEs given by

$$\begin{aligned}\dot{X} &= k_1AY - k_2XY + k_3AX - 2k_4X^2, & \dot{Y} &= -k_1AY - k_2XY + 1/2k_c fBZ, \\ \dot{Z} &= 2k_3AX - k_cBZ,\end{aligned}$$

which are typically scaled as [69]

$$\epsilon(dx/d\tau) = qy - xy + x(1 - x), \quad \epsilon'(dy/d\tau) = -qy - xy + fz, \quad dz/d\tau = x - z.$$

The basic chemistry of the BZ–oscillations involves jumps between high and low HBrO_2 (X) states, which is reflected in the relaxation oscillator nature of the Oregonator. This fundamental bistability may be stabilized in a flow reactor (CSTR) with reactants and Br^- in the feed stream. Hysteresis between the two states is observed both experimentally and in the Oregonator. Quasiperiodicity and chaos also are observed in CSTR and can be modeled by the Oregonator [10].

2.3.2 Multi–phase tumor growth equations

Our last reaction–diffusion system is a general model of multi–phase tumor growth, in the form of nonlinear parabolic PDE, as reviewed recently in [64]

$$\partial_t \Phi_i = \nabla \cdot (D_i \Phi_i) - \nabla \cdot (\mathbf{v}_i \Phi_i) + \lambda_i(\Phi_i, C_i) - \mu_i(\Phi_i, C_i) \quad (30)$$

($\partial_t \equiv \partial/\partial t$), where for phase i , Φ_i is the volume fraction ($\sum_i \Phi_i = 1$), D_i is the random motility or diffusion, $\lambda_i(\Phi_i, C_i)$ is the chemical and phase dependent production, and $\mu_i(\Phi_i, C_i)$ is the chemical and phase dependent degradation/death, and \mathbf{v}_i is the cell velocity defined by the constitutive equation

$$\mathbf{v}_i = -\mu \nabla p, \quad (31)$$

where μ is a positive constant describing the viscous–like properties of tumor cells and p is the spheroid internal pressure.

In particular, the multi–phase equation (30) splits into two heat–like mass–conservation PDEs [64],

$$\partial_t \Phi^C = S^C - \nabla \cdot (\mathbf{v}^C \Phi^C), \quad \partial_t \Phi^F = S^F - \nabla \cdot (\mathbf{v}^F \Phi^F), \quad (32)$$

where Φ^C and Φ^F are the tissue cell/matrix and fluid volume fractions, respectively, \mathbf{v}^C and \mathbf{v}^F are the cell/matrix and the fluid velocities (both defined by their constitutive

equations of the form of (31)), S^C is the rate of production of solid phase tumor tissue and S^F is the creation/degradation of the fluid phase. Conservation of matter in the tissue, $\Phi^C + \Phi^F = 1$, implies that $\nabla \cdot (\mathbf{v}^C \Phi^C + \mathbf{v}^F \Phi^F) = \Phi^C + \Phi^F$. The assumption that the tumor may be described by two phases only implies that the new cell/matrix phase is formed from the fluid phase and vice versa, so that $S^C + S^F = 0$. The detailed biochemistry of tumor growth can be coupled into the model above through the growth term S^C , with equations added for nutrient diffusion, see [64] and references therein.

The multi-phase tumor growth model (30) has been derived from the classical transport/mass conservation equations for different chemical species [64],

$$\partial_t u_i = P_i - \nabla \cdot \mathbf{N}_i. \quad (33)$$

Here C_i are the concentrations of the chemical species, subindex a for oxygen, b for glucose, c for lactate ion, d for carbon dioxide, e for bicarbonate ion, f for chloride ion, and g for hydrogen ion concentration; P_i is the net rate of consumption/production of the chemical species both by tumor cells and due to the chemical reactions with other species; and \mathbf{N}_i is the flux of each of the chemical species inside the tumor spheroid, given (in the simplest case of uncharged molecules of glucose, O_2 and CO_2) by Fick's law,

$$\mathbf{N}_i = -D_i \nabla u_i,$$

where D_i are (positive) constant diffusion coefficients. In case of charged molecules of ionic species, the flux \mathbf{N}_i contains also the (negative) gradient of the volume fractions Φ_i .

There are three distinct stages to cancer development: avascular, vascular, and metastatic – researchers often concentrate their efforts on answering specific OUPC-related questions on each of these stages [64]. In particular, as some tumor cell lines grown in vitro form spherical aggregates, the relative cheapness and ease of in vitro experiments in comparison to animal experiments has made 3D *multicellular tumor spheroids* (MTS, see Figure 6 in [64]) very popular in vitro model system of avascular tumors¹² [45]. They are used to study how local micro-environments affect cellular growth/decay, viability, and therapeutic response [66]. MTS provide, allowing strictly controlled nutritional and mechanical conditions, excellent experimental patterns to test the validity of the proposed mathematical models of tumor growth/decay [60].

¹²In vitro cultivation of tumor cells as multicellular tumor spheroids (MTS) has greatly contributed to the understanding of the role of the cellular micro-environment in tumor biology (for review see [66, 45]). These spherical cell aggregates mimic avascular tumor stages or micro-metastases in many aspects and have been studied intensively as an experimental model reflecting an in vivo-like micro-milieu with 3D metabolic gradients. With increasing size, most MCTS not only exhibit proliferation gradients from the periphery towards the center but they also develop a spheroid type-specific nutrient supply pattern, such as radial oxygen partial pressure gradients. Similarly, MCTS of a variety of tumor cell lines exhibit a concentric histo-morphology, with a necrotic core surrounded by a viable cell rim. The spherical symmetry is an important prerequisite for investigating the effect of environmental factors on cell proliferation and viability in a 3D environment on a quantitative basis.

3 Dissipative evolution under the Ricci flow

In this section we will derive the geometric formalism associated with the quadratic Ricci-flow equation (4), as a general framework for all presented bio-reaction-diffusion systems.

3.1 Geometrization Conjecture

Geometry and topology of smooth surfaces are related by the *Gauss-Bonnet formula* for a closed surface Σ (see, e.g., [31, 34])

$$\frac{1}{2\pi} \iint_{\Sigma} K dA = \chi(\Sigma) = 2 - 2 \text{gen}(\Sigma), \quad (34)$$

where dA is the area element of a metric g on Σ , K is the Gaussian curvature, $\chi(\Sigma)$ is the Euler characteristic of Σ and $\text{gen}(\Sigma)$ is its *genus*, or number of handles, of Σ . Every closed surface Σ admits a metric of constant Gaussian curvature $K = +1, 0$, or -1 and so is uniformized by elliptic, Euclidean, or hyperbolic geometry, which respectively have $\text{gen}(S^2) = 0$ (sphere), $\text{gen}(T^2) = 1$ (torus) and $\text{gen}(\Sigma) > 1$ (torus with several holes). The integral (34) is a *topological invariant* of the surface Σ , always equal to 2 for all topological spheres S^2 (that is, for all closed surfaces without holes that can be continuously deformed from the geometric sphere) and always equal to 0 for the topological torus T^2 (i.e., for all closed surfaces with one hole or handle).

Topological framework for the Ricci flow (2) is Thurston's *Geometrization Conjecture* [67], which states that the interior of any compact 3-manifold can be split in an essentially unique way by disjoint embedded 2-spheres S^2 and tori T^2 into pieces and each piece admits one of 8 geometric structures (including (i) the 3-sphere S^3 with constant curvature $+1$; (ii) the Euclidean 3-space \mathbb{R}^3 with constant curvature 0 and (iii) the hyperbolic 3-space \mathbb{H}^3 with constant curvature -1).¹³ The geometrization conjecture (which has the Poincaré Conjecture as a special case) would give us a link between the geometry and topology of 3-manifolds, analogous in spirit to the case of 2-surfaces.

In higher dimensions, the Gaussian curvature K corresponds to the Riemann curvature tensor \mathfrak{Rm} on a smooth n -manifold M , which is in local coordinates on M denoted by

¹³Another five allowed geometric structures are represented by the following examples: (iv) the product $S^2 \times S^1$; (v) the product $\mathbb{H}^2 \times S^1$ of hyperbolic plane and circle; (vi) a left invariant Riemannian metric on the special linear group $SL(2, \mathbb{R})$; (vii) a left invariant Riemannian metric on the solvable Poincaré-Lorentz group $E(1, 1)$, which consists of rigid motions of a $(1 + 1)$ -dimensional space-time provided with the flat metric $dt^2 - dx^2$; (viii) a left invariant metric on the nilpotent Heisenberg group, consisting of 3×3 matrices of the form

$$\begin{bmatrix} 1 & * & * \\ 0 & 1 & * \\ 0 & 0 & 1 \end{bmatrix}.$$

In each case, the universal covering of the indicated manifold provides a canonical model for the corresponding geometry [50].

its $(4, 0)$ -components R_{ijkl} , or its $(3, 1)$ -components R_{ijk}^l (see Appendix, as well as e.g., [31, 34]). The trace (or, contraction) of \mathfrak{Rm} , using the inverse metric tensor $g^{ij} = (g_{ij})^{-1}$, is the Ricci tensor \mathfrak{Rc} , the 3-dimensional curvature tensor, which is in a local coordinate system $\{x^i\}_{i=1}^n$ defined in an open set $U \subset M$, given by

$$R_{ij} = \text{tr}(\mathfrak{Rm}) = g^{kl} R_{ijkl}$$

(using Einstein's summation convention), while the *scalar curvature* is now given by the second contraction of \mathfrak{Rm} as

$$R = \text{tr}(\mathfrak{Rc}) = g^{ij} R_{ij}.$$

In general, the Ricci flow $g_{ij}(t)$ is a one-parameter family of Riemannian metrics on a compact n -manifold M governed by the equation (2), which has a unique solution for a short time for an arbitrary smooth metric g_{ij} on M [16]. If $\mathfrak{Rc} > 0$ at any local point $x = \{x^i\}$ on M , then the Ricci flow (2) contracts the metric $g_{ij}(t)$ near x , to the future, while if $\mathfrak{Rc} < 0$, then the flow (2) expands $g_{ij}(t)$ near x . The solution metric $g_{ij}(t)$ of the Ricci flow equation (2) shrinks in positive Ricci curvature direction while it expands in the negative Ricci curvature direction, because of the minus sign in the front of the Ricci tensor R_{ij} . In particular, on a 2-sphere S^2 , any metric of positive Gaussian curvature will shrink to a point in finite time. At a general point, there will be directions of positive and negative Ricci curvature along which the metric will locally contract or expand (see [4]). Also, if a simply-connected compact 3-manifold M has a Riemannian metric g_{ij} with positive Ricci curvature then it is diffeomorphic to the 3-sphere S^3 [16].

3.2 Reaction-diffusion-type evolution of curvatures and volumes

All three Riemannian curvatures (R , \mathfrak{Rc} and \mathfrak{Rm}), as well as the associated volume forms, *evolve* during the Ricci flow (2). In general, the Ricci-flow evolution equation (2) for the metric tensor g_{ij} implies the reaction-diffusion-type evolution equation for the Riemann curvature tensor \mathfrak{Rm} on an n -manifold M ,

$$\partial_t \mathfrak{Rm} = \Delta \mathfrak{Rm} + Q_n, \tag{35}$$

where Q_n is a quadratic expression of the Riemann n -curvatures, corresponding to the n -component bio-chemical reaction, while the term $\Delta \mathfrak{Rm}$ corresponds to the n -component diffusion. From the general n -curvature evolution (35) we have two important particular cases:¹⁴

¹⁴By expanding the maximum principle for tensors, Hamilton proved that Ricci flow $g(t)$ given by (2) preserves the positivity of the Ricci tensor \mathfrak{Rc} on 3-manifolds (as well as of the Riemann curvature tensor \mathfrak{Rm} in all dimensions); moreover, the eigenvalues of the Ricci tensor on 3-manifolds (and of the curvature operator \mathfrak{Rm} on 4-manifolds) are getting pinched point-wisely as the curvature is getting large [16, 17]. This

1. The evolution equation for the Ricci curvature tensor $\mathfrak{R}\mathfrak{c}$ on a 3-manifold M ,

$$\partial_t \mathfrak{R}\mathfrak{c} = \Delta \mathfrak{R}\mathfrak{c} + Q_3, \quad (36)$$

where Q_3 is a quadratic expression of the Ricci 3-curvatures, corresponding to the 3-component bio-chemical reaction, while the term $\Delta \mathfrak{R}\mathfrak{c}$ corresponds to the 3-diffusion.

2. The evolution equation for the scalar 2-surface curvature R ,

$$\partial_t R = \Delta R + 2|\mathfrak{R}\mathfrak{c}|^2, \quad (37)$$

(which holds both on any 3-manifold M and on its boundary 2-surface ∂M), in which the term $2|\mathfrak{R}\mathfrak{c}|^2$ corresponds to the 2-component bio-chemical reaction, while the term ΔR corresponds to the 2-component diffusion. By the *maximum principle* (see subsection 3.4), the minimum of the scalar curvature R is non-decreasing along the flow $g(t)$, both on M and on ∂M (see [58]).

Let us now see in detail how various geometric quantities evolve given the *short-time solution* of the Ricci flow equation (2) on an arbitrary n -manifold M . For this, we need first to calculate the *variation formulas* for the Christoffel symbols and curvature tensors on M ; then the corresponding evolution equations will naturally follow (see [16, 7, 8]). If $g(s)$ is a 1-parameter family of metrics on M with $\partial_s g_{ij} = v_{ij}$, then the variation of the Christoffel symbols Γ_{ij}^k on M is given by

$$\partial_s \Gamma_{ij}^k = \frac{1}{2} g^{kl} (\nabla_i v_{jl} + \nabla_j v_{il} - \nabla_l v_{ij}), \quad (38)$$

from which follows the evolution of the Christoffel symbols Γ_{ij}^k under the Ricci flow $g(t)$ on M given by (2),

$$\partial_t \Gamma_{ij}^k = -g^{kl} (\nabla_i R_{jl} + \nabla_j R_{il} - \nabla_l R_{ij}).$$

From (38) we calculate the variation of the Ricci tensor R_{ij} on M as

$$\partial_s R_{ij} = \nabla_m (\partial_s \Gamma_{ij}^m) - \nabla_i (\partial_s \Gamma_{mj}^m), \quad (39)$$

and the variation of the scalar curvature R on M by

$$\partial_s R = -\Delta V + \operatorname{div}(\operatorname{div} v) - \langle v, \mathfrak{R}\mathfrak{c} \rangle, \quad (40)$$

observation allowed him to prove the convergence results: the evolving metrics (on a compact manifold) of positive Ricci curvature in dimension 3 (or positive Riemann curvature in dimension 4) converge, modulo scaling, to metrics of constant positive curvature.

However, without assumptions on curvature, the long time behavior of the metric evolving by Ricci flow may be more complicated [58]. In particular, as t approaches some finite time T , the curvatures may become arbitrarily large in some region while staying bounded in its complement. On the other hand, Hamilton [19] discovered a remarkable property of solutions with nonnegative curvature tensor $\mathfrak{R}\mathfrak{m}$ in arbitrary dimension, called the *differential Harnack inequality*, which allows, in particular, to compare the curvatures of the solution of (2) at different points and different times.

where $V = g^{ij}v_{ij} = \text{tr}(v)$ is the trace of $v = (v_{ij})$.

If an n -manifold M is oriented, then the *volume* n -form on M is given, in a positively-oriented local coordinate system $\{x^i\} \in U \subset M$, by [29]

$$d\mu = \sqrt{\det(g_{ij})} dx^1 \wedge dx^2 \wedge \dots \wedge dx^n. \quad (41)$$

If $\partial_s g_{ij} = v_{ij}$, then $\partial_s d\mu = \frac{1}{2}Vd\mu$. The evolution of the volume n -form $d\mu$ under the Ricci flow $g(t)$ on M is given by the exponential decay/growth relation with the scalar curvature R as the rate constant,

$$\partial_t d\mu = -Rd\mu, \quad (42)$$

which gives an exponential decay for $R > 0$ (elliptic geometry) and exponential growth for $R < 0$ (hyperbolic geometry). The elementary volume evolution (42) implies the integral form of the exponential relation for the total n -volume

$$\text{vol}(g) = \int_M d\mu, \quad \text{as} \quad \partial_t \text{vol}(g(t)) = - \int_M Rd\mu,$$

which again gives an *exponential decay* for elliptic $R > 0$ and *exponential growth* for hyperbolic $R < 0$.

This is a crucial point for the *tumor suppression* by the body: the immune system needs to keep the elliptic geometry of the MTS, evolving by (30) – by all possible means.¹⁵ In the healthy organism this normally happens, because the initial MTS started as a spherical shape with $R > 0$. The immune system just needs to keep the MTS in the spherical/elliptic shape and prevent any hyperbolic distortions of $R < 0$. Thus, it will naturally have an exponential decay and vanish.

Since the n -volume is not constant and sometimes we would like to prevent the solution from shrinking to an n -point on M (elliptic case) or expanding to an infinity (hyperbolic case), we can also consider the *normalized Ricci flow* on M (see Figure 1 as well as ref. [7]):

$$\partial_t \hat{g}_{ij} = -2\hat{R}_{ij} + \frac{2}{n}\hat{r}\hat{g}_{ij}, \quad \text{where} \quad \hat{r} = \text{vol}(\hat{g})^{-1} \int_M \hat{R}d\mu \quad (43)$$

¹⁵As a tumor decay control tool, a monoclonal antibody therapy is usually proposed. Monoclonal antibodies (mAb) are mono-specific antibodies that are identical because they are produced by one type of immune cell that are all clones of a single parent cell. Given (almost) any substance, it is possible to create monoclonal antibodies that specifically bind to that substance; they can then serve to detect or purify that substance. The invention of monoclonal antibodies is generally accredited to Georges Köhler, César Milstein, and Niels Kaj Jerne in 1975 [42], who shared the Nobel Prize in Physiology or Medicine in 1984 for the discovery. The key idea was to use a line of myeloma cells that had lost their ability to secrete antibodies, come up with a technique to fuse these cells with healthy antibody producing B-cells, and be able to select for the successfully fused cells.

is the average scalar curvature on M . We then have the n -volume conservation law:

$$\partial_t \text{vol}(\hat{g}(t)) = 0.$$

To study the *long-time existence* of the normalized Ricci flow (43) on an arbitrary n -manifold M , it is important to know what kind of curvature conditions are preserved under the equation. In general, the Ricci flow $g(t)$ on M , as defined by the fundamental relation (2), tends to preserve some kind of positivity of curvatures. For example, positive scalar curvature R (i.e., elliptic geometry) is preserved both on M and on its boundary ∂M in any dimension. This follows from applying the maximum principle to the evolution equation (37) for scalar curvature R both on M and on ∂M . Similarly, positive Ricci curvature is preserved under the Ricci flow on a 3-manifold M . This is a special feature of dimension 3 and is related to the fact that the Riemann curvature tensor may be recovered algebraically from the Ricci tensor and the metric on 3-manifolds [7].

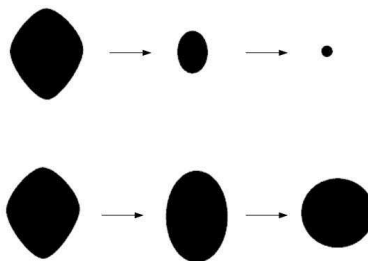


Figure 1: An example of Ricci flow normalization: unnormalized flow (up) and normalized flow (down).

In particular, we have the following result for 2-surfaces (see [18]): Let $S = \partial M$ be a closed 2-surface, which is a boundary of a compact 3-manifold M . Then for any initial 2-metric g_0 on ∂M , the solution to the normalized Ricci flow (43) on ∂M exists for all time. Moreover, (i) if the Euler characteristic of ∂M is non-positive, then the solution metric $g(t)$ on ∂M converges to a constant curvature metric as $t \rightarrow \infty$; and (ii) if the scalar curvature R of the initial metric g_0 is positive, then the solution metric $g(t)$ on ∂M converges to a positive constant curvature metric as $t \rightarrow \infty$. (For surfaces with non-positive Euler characteristic, the proof is based primarily on maximum principle estimates for the scalar curvature.)

Applying to the tumor evolution (30), the normalized Ricci flow (43) of the MTS will make it completely round with a geometric sphere shell, which is ideal for surgical removal. This is our second option for the MTS growth/decay control. If we cannot force it to exponential decay, then we must try to normalize into a round spherical shell – which is suitable for surgical removal.

The negative flow of the total n -volume $\text{vol}(g(t))$ represents the *Einstein–Hilbert functional* (see [51, 7, 4])

$$E(g) = \int_M R d\mu = -\partial_t \text{vol}(g(t)).$$

If we put $\partial_s g_{ij} = v_{ij}$, we have

$$\partial_s E(g) = \int_M \left(-\Delta V + \text{div}(\text{div } v) - \langle v, \mathfrak{Rc} \rangle + \frac{1}{2} R V \right) d\mu = \int_M \left\langle v, \frac{1}{2} R g_{ij} - R_{ij} \right\rangle d\mu,$$

so, the critical points of $E(g)$ satisfy *Einstein's equation* $\frac{1}{2} R g_{ij} = R_{ij}$ in the vacuum. The gradient flow of $E(g)$ on an n -manifold M ,

$$\partial_t g_{ij} = 2 (\nabla E(g))_{ij} = R g_{ij} - 2 R_{ij},$$

is the Ricci flow (2) plus $R g_{ij}$. Thus, Einstein metrics are the fixed points of the Ricci flow $g(t)$ on M .¹⁶

Let Δ denote the Laplacian acting on functions on an arbitrary n -manifold M , which is in local coordinates $\{x^i\} \in U \subset M$ given by

$$\Delta = g^{ij} \nabla_i \nabla_j = g^{ij} \left(\partial_{ij} - \Gamma_{ij}^k \partial_k \right).$$

For any smooth function f on M we have [16, 8]

$$\Delta \nabla_i f = \nabla_i \Delta f + R_{ij} \nabla_j f \quad \text{and} \quad \Delta |\nabla f|^2 = 2 |\nabla_i \nabla_j f|^2 + 2 R_{ij} \nabla_i f \nabla_j f + 2 \nabla_i f \nabla_i \Delta f,$$

from which it follows that if we have

$$\begin{aligned} \mathfrak{Rc} &\geq 0, & \Delta f &\equiv 0, & |\nabla f| &\equiv 1, & \text{then} \\ \nabla \nabla f &\equiv 0 & \text{and} & & \mathfrak{Rc}(\nabla f, \nabla f) &\equiv 0. \end{aligned}$$

Using this Laplacian Δ , we can write the linear heat equation on M as $\partial_t u = \Delta u$, where u is the temperature. In particular, the Laplacian acting on functions with respect to $g(t)$ will be denoted by $\Delta_{g(t)}$. If $(M, g(t))$ is a solution to the Ricci flow equation (2), then we have

$$\partial_t \Delta_{g(t)} = 2 R_{ij} \nabla_i \nabla_j.$$

In particular, the evolution equation (37) for the scalar 2-curvature R under the Ricci flow (2) follows from (40). Using equation (53) from Appendix, we have:

$$\text{div}(\mathfrak{Rc}) = \frac{1}{2} \nabla R, \quad \text{so that} \quad \text{div}(\text{div}(\mathfrak{Rc})) = \frac{1}{2} \Delta R,$$

¹⁶Einstein metrics on n -manifolds are metrics with constant curvature. However, along the way, the deformation will encounter singularities. The major question, resolved by Perelman, was how to find a way to describe all possible singularities.

showing again that the scalar curvature R satisfies a heat-type equation with a quadratic nonlinearity both on a 3-manifold M and on its boundary 2-surface ∂M .

Next we will find the exact form of the evolution equation (36) for the Ricci tensor \mathfrak{Rc} under the Ricci flow $g(t)$ given by (2) on any 3-manifold M . (Note that in higher dimensions, the appropriate formula of huge complexity would involve the whole Riemann curvature tensor \mathfrak{Rm} .) Given a variation $\partial_s g_{ij} = v_{ij}$, from (39) we get

$$\partial_s R_{ij} = \frac{1}{2} (\Delta_L v_{ij} + \nabla_i \nabla_j V - \nabla_i (\operatorname{div} v)_j - \nabla_j (\operatorname{div} v)_i),$$

where Δ_L denotes the so-called Lichnerowicz Laplacian (which depends on \mathfrak{Rm} , see [16, 8]). Since

$$\nabla_i \nabla_j R - \nabla_i (\operatorname{div}(\mathfrak{Rc}))_j - \nabla_j (\operatorname{div}(\mathfrak{Rc}))_i = 0,$$

by (53) (after some algebra) we get that under the Ricci flow (2) the evolution equation for the Ricci tensor \mathfrak{Rc} on a 3-manifold M is

$$\partial_t R_{ij} = \Delta R_{ij} + 3R R_{ij} - 6R_{im} R_{jm} + (2|\mathfrak{Rc}|^2 - R^2) g_{ij}.$$

So, just as in case of the evolution (37) of the scalar curvature $\partial_t R$ (both on a 3-manifold M and on its 2-boundary ∂M), we get a heat-type evolution equation with a quadratic nonlinearity for $\partial_t R_{ij}$, which means that positive Ricci curvature ($\mathfrak{Rc} > 0$) of elliptic 3-geometry is preserved under the Ricci flow $g(t)$ on M .

More generally, we have the following result for 3-manifolds (see [16]): Let (M, g_0) be a compact Riemannian 3-manifold with positive Ricci curvature \mathfrak{Rc} . Then there exists a unique solution to the normalized Ricci flow $g(t)$ on M with $g(0) = g_0$ for all time and the metrics $g(t)$ converge exponentially fast to a constant positive sectional curvature metric g_∞ on M . In particular, M is diffeomorphic to a 3-sphere S^3 . (As a consequence, such a 3-manifold M is necessarily diffeomorphic to a quotient of the 3-sphere by a finite group of isometries. It follows that given any homotopy 3-sphere, if one can show that it admits a metric with positive Ricci curvature, then the Poincaré Conjecture would follow [7].) In particular, compact and closed 3-manifolds which admit a non-singular solution can also be decomposed into geometric pieces [20].

From the geometric evolution equations reviewed in this subsection, we see that both short-time and long-time geometric solution can always be found for 2-component bio-reaction-diffusion equations, as they correspond to evolution of the scalar 2-curvature R . Regarding the 3-component bio-reaction-diffusion equations, corresponding to evolution of the Ricci 3-curvature \mathfrak{Rc} , we can always find the short-time geometric solution, while the long-time solution exists only under some additional (compactness and/or closure) conditions. Finally, in case of n -component bio-reaction-diffusion equations, corresponding to evolution of the Riemann n -curvature \mathfrak{Rm} , only short-time geometric solution is possible.

3.3 Dissipative solitons and Ricci breathers

An important class of bio–reaction–diffusion systems are *dissipative solitons* (DSs), which are stable solitary localized structures that arise in nonlinear spatially extended dissipative systems due to mechanisms of *self–organization*. They can be considered as an extension of the classical soliton concept in conservative systems. Apart from aspects similar to the behavior of classical particles like the formation of bound states, DSs exhibit entirely nonclassical behavior – e.g., scattering, generation and annihilation – all without the constraints of energy or momentum conservation. The excitation of internal degrees of freedom may result in a dynamically stabilized intrinsic speed, or periodic oscillations of the shape.

In particular, stationary DSs are generated by production of material in the center of the DSs, diffusive transport into the tails and depletion of material in the tails. A propagating pulse arises from production in the leading and depletion in the trailing end. Among other effects, one finds periodic oscillations of DSs, the so–called ‘breathing’ dissipative solitons [15].

DSs in many different systems show universal particle–like properties. To understand and describe the latter, one may try to derive ‘particle equations’ for slowly varying order parameters like position, velocity or amplitude of the DSs by adiabatically eliminating all fast variables in the field description. This technique is known from linear systems, however mathematical problems arise from the nonlinear models due to a coupling of fast and slow modes [13].

Similar to low–dimensional dynamic systems, for supercritical bifurcations of stationary DSs one finds characteristic normal forms essentially depending on the symmetries of the system; e.g., for a transition from a symmetric stationary to an intrinsically propagating DS one finds the Pitchfork normal form for the DS–velocity \mathbf{v} [6],

$$\dot{\mathbf{v}} = (\sigma - \sigma_0)\mathbf{v} - |\mathbf{v}|^2\mathbf{v}$$

where σ represents the bifurcation parameter and σ_0 the bifurcation point. For a bifurcation to a ‘breathing’ DS, one finds the Hopf normal form [32]

$$\dot{A} = (\sigma - \sigma_0)A - |A|^2A$$

for the amplitude A of the oscillation. Note that the above problems do not arise for classical solitons as inverse scattering theory yields complete analytical solutions [15].

3.3.1 Ricci breathers and Ricci solitons

Closely related to dissipative solitons are the so–called *breathers*, solitonic structures given by localized periodic solutions of some nonlinear soliton PDEs, including the exactly–

solvable sine–Gordon equation¹⁷ and the focusing nonlinear Schrödinger equation.¹⁸

A metric $g_{ij}(t)$ evolving by the Ricci flow $g(t)$ given by (2) on any 3–manifold M is called a *Ricci breather*, if for some $t_1 < t_2$ and $\alpha > 0$ the metrics $\alpha g_{ij}(t_1)$ and $g_{ij}(t_2)$ differ only by a diffeomorphism; the cases $\alpha = 1, \alpha < 1, \alpha > 1$ correspond to steady, shrinking and expanding breathers, respectively. Trivial breathers on M , for which the metrics $g_{ij}(t_1)$ and $g_{ij}(t_2)$ differ only by diffeomorphism and scaling for each pair of t_1 and t_2 , are called *Ricci solitons*. Thus, if one considers Ricci flow as a dynamical system on the space of Riemannian metrics modulo diffeomorphism and scaling, then breathers and solitons correspond to periodic orbits and fixed points respectively. At each time the Ricci soliton metric satisfies on M an equation of the form [58]

$$R_{ij} + c g_{ij} + \nabla_i b_j + \nabla_j b_i = 0,$$

where c is a number and b_i is a 1–form; in particular, when $b_i = \frac{1}{2} \nabla_i a$ for some function a on M , we get a gradient Ricci soliton. An important example of a gradient shrinking soliton is the *Gaussian soliton*, for which the metric g_{ij} is just the Euclidean metric on \mathbb{R}^3 , $c = 1$ and $a = -|x|^2/2$.

3.4 Smoothing heat equation and Ricci entropy

Given a C^2 function $u : M \rightarrow \mathbb{R}$ on a Riemannian 3–manifold M , its Laplacian is defined in local coordinates $\{x^i\} \in U \subset M$ to be

$$\Delta u = \text{tr}_g (\nabla^2 u) = g^{ij} \nabla_i \nabla_j u,$$

where ∇_i is the *covariant derivative* (Levi–Civita connection, see Appendix). We say that a C^2 function $u : M \times [0, T) \rightarrow \mathbb{R}$, where $T \in (0, \infty]$, is a solution to the heat

¹⁷An exact solution $u = u(x, t)$ of the (1+1)D sine–Gordon equation

$$\begin{aligned} \partial_{t^2} u &= \partial_{x^2} u - \sin u, \quad \text{is [1]} \\ u &= 4 \arctan \left(\frac{\sqrt{1-\omega^2} \cos(\omega t)}{\omega \cosh(\sqrt{1-\omega^2} x)} \right), \end{aligned}$$

which, for $\omega < 1$, is periodic in time t and decays exponentially when moving away from $x = 0$.

¹⁸The focusing nonlinear Schrödinger equation is the dispersive complex–valued (1+1)D PDE [2],

$$i \partial_t u + \partial_{x^2} u + |u|^2 u = 0,$$

with a breather solution of the form:

$$u = \left(\frac{2b^2 \cosh(\theta) + 2ib\sqrt{2-b^2} \sinh(\theta)}{2 \cosh(\theta) - \sqrt{2}\sqrt{2-b^2} \cos(abx)} - 1 \right) a \exp(i a^2 t) \quad \text{with} \quad \theta = a^2 b \sqrt{2-b^2} t,$$

which gives breathers periodic in space x and approaching the uniform value a when moving away from the focus time $t = 0$.

equation if (3) holds. One of the most important properties satisfied by the heat equation is the *maximum principle*, which says that for any smooth solution to the heat equation, whatever point-wise bounds hold at $t = 0$ also hold for $t > 0$ [7]. More precisely, we can state: Let $u : M \times [0, T) \rightarrow \mathbb{R}$ be a C^2 solution to the heat equation (3) on a complete Riemannian 3-manifold M . If $C_1 \leq u(x, 0) \leq C_2$ for all $x \in M$, for some constants $C_1, C_2 \in \mathbb{R}$, then $C_1 \leq u(x, t) \leq C_2$ for all $x \in M$ and $t \in [0, T)$. This property exhibits the smoothing behavior of the heat equation (3) on M .

Now, consider Perelman's *entropy functional* [58] on a 3-manifold M ¹⁹

$$\mathcal{F} = \int_M (R + |\nabla f|^2) e^{-f} d\mu \quad (44)$$

for a Riemannian metric g_{ij} and a (temperature-like) scalar function f on a closed 3-manifold M , where $d\mu$ is the volume 3-form (41). During the Ricci flow (2), \mathcal{F} evolves on M as

$$\partial_t \mathcal{F} = 2 \int_M |R_{ij} + \nabla_i \nabla_j f|^2 e^{-f} d\mu. \quad (45)$$

Now, define $\lambda(g_{ij}) = \inf \mathcal{F}(g_{ij}, f)$, where infimum is taken over all smooth f , satisfying

$$\int_M e^{-f} d\mu = 1. \quad (46)$$

$\lambda(g_{ij})$ is the lowest eigenvalue of the operator $-4\Delta + R$. Then the entropy evolution formula (45) implies that $\lambda(g_{ij}(t))$ is nondecreasing in t , and moreover, if $\lambda(t_1) = \lambda(t_2)$, then for $t \in [t_1, t_2]$ we have $R_{ij} + \nabla_i \nabla_j f = 0$ for f which minimizes \mathcal{F} on M [58]. Thus a steady breather on M is necessarily a steady soliton.

If we define the conjugate *heat operator* on M as

$$\square^* = -\partial/\partial t - \Delta + R$$

then we have the *conjugate heat equation*²⁰ [58]

$$\square^* u = 0. \quad (48)$$

¹⁹Note that in the related context of Riemannian gravitation theory, the so-called *gravitational entropy* is embedded in the Weyl curvature (4, 0)-tensor \mathfrak{W} , which is the traceless component of the Riemann curvature tensor \mathfrak{Rm} (i.e., \mathfrak{Rm} with the Ricci tensor \mathfrak{Rc} removed),

$$\mathfrak{W} = \mathfrak{Rm} - f(R_{ij}g_{ij}),$$

where $f(R_{ij}g_{ij})$ is a certain linear function of R_{ij} and g_{ij} . According to Penrose's *Weyl curvature hypothesis*, the entire *history of a closed universe* starts from a uniform low-entropy Big Bang with zero Weyl curvature tensor of the cosmological gravitational field and ends with a high-entropy Big Crunch, representing the congealing of many black holes, with Weyl tensor approaching infinity (see [57, 27]).

²⁰In [58] Perelman stated a differential Li-Yau-Hamilton (LYH) type inequality [28] for the fundamental solution $u = u(x, t)$ of the conjugate heat equation (48) on a closed n -manifold M evolving by the Ricci

The entropy functional (44) is nondecreasing under the coupled *Ricci-diffusion flow* on M (see [72, 47])

$$\partial_t g_{ij} = -2R_{ij}, \quad \partial_t u = -\Delta u + \frac{R}{2}u - \frac{|\nabla u|^2}{u}, \quad (49)$$

where the second equation ensures $\int_M u^2 d\mu = 1$, to be preserved by the Ricci flow $g(t)$ on M . If we define $u = e^{-\frac{f}{2}}$, then the right-hand equation in (49) is equivalent to the generic scalar-field f -evolution equation on M ,

$$\partial_t f = -\Delta f - R + |\nabla f|^2,$$

which instead preserves (46).

The coupled Ricci-diffusion flow (49), or equivalently, the dual system

$$\partial_t g_{ij} = \Delta_M g_{ij} + Q_{ij}(g, \partial g), \quad \partial_t f = -\Delta f - R + |\nabla f|^2, \quad (50)$$

is our *global decay* model for a general n -dimensional bio-reaction-diffusion process, including both geometric and bio-chemical multi-phase evolution.

The sole *hypothesis of this paper* is that any kind of reaction-diffusion processes in biology, chemistry and physics is subsumed by the geometric-diffusion system (49), or the dual system (50).

flow (2). Let $p \in M$ and

$$u = (4\pi\tau)^{-\frac{n}{2}} e^{-f}$$

be the fundamental solution of the conjugate heat equation in $M \times (0, T)$,

$$\square^* u = 0, \quad \text{or} \quad \partial_t u + \Delta u = Ru,$$

where $\tau = T - t$ and $R = R(\cdot, t)$ is the scalar curvature of M with respect to the metric $g(t)$ with $\lim_{t \nearrow T} u = \delta_p$ (in the distribution sense), where δ_p is the delta-mass at p . Let

$$v = [\tau(2\Delta f - |\nabla f|^2 + R) + f - n]u,$$

where $\tau = T - t$. Then we have a differential LYH-type inequality

$$v(x, t) \leq 0 \quad \text{in} \quad M \times (0, T). \quad (47)$$

This result was used by Perelman to give a proof of the *pseudolocality theorem* [58] which roughly said that almost Euclidean regions of large curvature in closed manifold with metric evolving by Ricci flow $g(t)$ given by (2) remain localized.

In particular, let $(M, g(t))$, $0 \leq t \leq T$, $\partial M \neq \emptyset$, be a compact 3-manifold with metric $g(t)$ evolving by the Ricci flow $g(t)$ given by (2) such that the second fundamental form of the surface ∂M with respect to the unit outward normal $\partial/\partial\nu$ of ∂M is uniformly bounded below on $\partial M \times [0, T]$. A global Li-Yau gradient estimate [46] for the solution of the generalized conjugate heat equation was proved in [28] (using a variation of the method of P. Li and S.T. Yau, [46]) on such a manifold with Neumann boundary condition.

3.5 Thermodynamic analogy

Perelman's functional \mathcal{F} is analogous to negative entropy [58]. Recall that thermodynamic *partition function* for a generic canonical ensemble at temperature β^{-1} is given by

$$Z = \int e^{-\beta E} d\omega(E), \quad (51)$$

where $\omega(E)$ is a 'density measure', which does not depend on β . From it, the *average energy* is given by

$$\langle E \rangle = -\partial_\beta \ln Z,$$

the *entropy* is

$$S = \beta \langle E \rangle + \ln Z,$$

and the *fluctuation* is

$$\sigma = \langle (E - \langle E \rangle)^2 \rangle = \partial_{\beta^2} \ln Z.$$

If we now fix a closed 3-manifold M with a probability measure m and a metric $g_{ij}(\tau)$ that depends on the temperature τ , then according to equation

$$\partial_\tau g_{ij} = 2(R_{ij} + \nabla_i \nabla_j f),$$

the partition function (51) is given by

$$\ln Z = \int (-f + \frac{n}{2}) dm. \quad (52)$$

From (52) we get (see [58])

$$\begin{aligned} \langle E \rangle &= -\tau^2 \int_M (R + |\nabla f|^2 - \frac{n}{2\tau}) dm, \\ S &= - \int_M (\tau(R + |\nabla f|^2) + f - n) dm, \\ \sigma &= 2\tau^4 \int_M |R_{ij} + \nabla_i \nabla_j f - \frac{1}{2\tau} g_{ij}|^2 dm, \end{aligned}$$

where

$$dm = u dV, \quad u = (4\pi\tau)^{-\frac{n}{2}} e^{-f}.$$

From the above formulas, we see that the fluctuation σ is nonnegative; it vanishes only on a gradient shrinking soliton. $\langle E \rangle$ is nonnegative as well, whenever the flow exists for all sufficiently small $\tau > 0$. Furthermore, if the heat function u : (a) tends to a δ -function as $\tau \rightarrow 0$, or (b) is a limit of a sequence of partial heat functions u_i , such that each u_i tends to a δ -function as $\tau \rightarrow \tau_i > 0$, and $\tau_i \rightarrow 0$, then the entropy S is also nonnegative. In case (a), all the quantities $\langle E \rangle, S, \sigma$ tend to zero as $\tau \rightarrow 0$, while in case (b), which may be interesting if $g_{ij}(\tau)$ becomes singular at $\tau = 0$, the entropy S may tend to a positive limit.

4 Appendix

4.1 Riemann and Ricci curvatures on a smooth n -manifold

Recall that proper differentiation of vector and tensor fields on a smooth Riemannian n -manifold is performed using the *Levi-Civita covariant derivative* (see, e.g., [31, 34]). Formally, let M be a Riemannian n -manifold with the tangent bundle TM and a local coordinate system $\{x^i\}_{i=1}^n$ defined in an open set $U \subset M$. The covariant derivative operator, $\nabla_X : C^\infty(TM) \rightarrow C^\infty(TM)$, is the unique linear map such that for any vector fields X, Y, Z , constant c , and function f the following properties are valid:

$$\begin{aligned}\nabla_{X+cY} &= \nabla_X + c\nabla_Y, \\ \nabla_X(Y + fZ) &= \nabla_X Y + (Xf)Z + f\nabla_X Z, \\ \nabla_X Y - \nabla_Y X &= [X, Y],\end{aligned}$$

where $[X, Y]$ is the Lie bracket of X and Y (see, e.g., [29]). In local coordinates, the metric g is defined for any orthonormal basis $(\partial_i = \partial_{x^i})$ in $U \subset M$ by

$$g_{ij} = g(\partial_i, \partial_j) = \delta_{ij}, \quad \partial_k g_{ij} = 0.$$

Then the affine *Levi-Civita connection* is defined on M by

$$\nabla_{\partial_i} \partial_j = \Gamma_{ij}^k \partial_k, \quad \text{where} \quad \Gamma_{ij}^k = \frac{1}{2} g^{kl} (\partial_i g_{jl} + \partial_j g_{il} - \partial_l g_{ij})$$

are the (second-order) *Christoffel symbols*.

Now, using the covariant derivative operator ∇_X we can define the *Riemann curvature* $(3, 1)$ -tensor \mathfrak{Rm} by (see, e.g., [31, 34])

$$\mathfrak{Rm}(X, Y)Z = \nabla_X \nabla_Y Z - \nabla_Y \nabla_X Z - \nabla_{[X, Y]} Z.$$

\mathfrak{Rm} measures the curvature of the manifold by expressing how noncommutative covariant differentiation is. The $(3, 1)$ -components R_{ijk}^l of \mathfrak{Rm} are defined in $U \subset M$ by

$$\begin{aligned}\mathfrak{Rm}(\partial_i, \partial_j)\partial_k &= R_{ijk}^l \partial_l, \quad \text{which expands (see [51]) as} \\ R_{ijk}^l &= \partial_i \Gamma_{jk}^l - \partial_j \Gamma_{ik}^l + \Gamma_{jk}^m \Gamma_{im}^l - \Gamma_{ik}^m \Gamma_{jm}^l.\end{aligned}$$

Also, the Riemann $(4, 0)$ -tensor $R_{ijkl} = g_{lm} R_{ijk}^m$ is defined as the g -based inner product on M ,

$$R_{ijkl} = \langle \mathfrak{Rm}(\partial_i, \partial_j)\partial_k, \partial_l \rangle.$$

The first and second Bianchi identities for the Riemann $(4, 0)$ -tensor R_{ijkl} hold,

$$R_{ijkl} + R_{jkil} + R_{kijl} = 0, \quad \nabla_i R_{jklm} + \nabla_j R_{kilm} + \nabla_k R_{ijlm} = 0,$$

while the twice contracted second Bianchi identity reads

$$2\nabla_j R_{ij} = \nabla_i R. \quad (53)$$

The $(0, 2)$ Ricci tensor \mathfrak{Rc} is the trace of the Riemann $(3, 1)$ -tensor \mathfrak{Rm} ,

$$\mathfrak{Rc}(Y, Z) + \text{tr}(X \rightarrow \mathfrak{Rm}(X, Y)Z), \quad \text{so that} \quad \mathfrak{Rc}(X, Y) = g(\mathfrak{Rm}(\partial_i, X)\partial_i, Y),$$

Its components $R_{jk} = \mathfrak{Rc}(\partial_j, \partial_k)$ are given in $U \subset M$ by the contraction [51]

$$\begin{aligned} R_{jk} &= R_{ijk}^i, \quad \text{or, in terms of Christoffel symbols,} \\ R_{jk} &= \partial_i \Gamma_{jk}^i - \partial_k \Gamma_{ji}^i + \Gamma_{mi}^i \Gamma_{jk}^m - \Gamma_{mk}^i \Gamma_{ji}^m. \end{aligned}$$

Being a symmetric second-order tensor, \mathfrak{Rc} has $\binom{n+1}{2}$ independent components on an n -manifold M . In particular, on a 3-manifold, it has 6 components, and on a 2-surface it has only the following 3 components:

$$R_{11} = g^{22} R_{2112}, \quad R_{12} = g^{12} R_{2121}, \quad R_{22} = g^{11} R_{1221},$$

which are all proportional to the corresponding coordinates of the metric tensor,

$$\frac{R_{11}}{g_{11}} = \frac{R_{12}}{g_{12}} = \frac{R_{22}}{g_{22}} = -\frac{R_{1212}}{\det(g)}. \quad (54)$$

Finally, the scalar curvature R is the trace of the Ricci tensor \mathfrak{Rc} , given in $U \subset M$ by: $R = g^{ij} R_{ij}$.

For example, on a geometric 2-sphere, we have the following relation between Cartesian $(y^i, i = 1, 2, 3)$ and polar coordinates $(x^j, j = 1, 2)$:

$$y^1 = R \cos x^1 \cos x^2, \quad y^2 = R \sin x^1 \cos x^2, \quad y^3 = R \sin x^2,$$

and the components of the metric tensor are

$$\{g_{ij}\} = \begin{Bmatrix} R^2 \cos^2 x^2 & 0 \\ 0 & R^2 \end{Bmatrix}, \quad \det(g_{ij}) = R^4 \cos^2 x^2,$$

so that we have only one component of the Riemann tensor: $R_{1212} = R^2 \sin^2 x^2$. Next, from (54) we get the components of \mathfrak{Rc}

$$\begin{aligned} R_{11} &= -\sin^2 x^2, \quad R_{12} = R_{21} = 0, \quad R_{22} = -\tan^2 x^2, \quad \text{or} \\ \{R_{ij}\} &= \begin{Bmatrix} -\sin^2 x^2 & 0 \\ 0 & -\tan^2 x^2 \end{Bmatrix}. \end{aligned}$$

Finally, for the scalar Ricci curvature, $R = g^{ij} R_{ij}$, we have

$$R = g^{11} R_{11} + g^{22} R_{22} = -\frac{2}{R^2} \tan^2 x^2.$$

Similarly, on a Riemannian n -manifold M of constant Gaussian curvature K , Ricci tensor is proportional to the metric tensor, $R_{ij} = -(n-1)K g_{ij}$, while Ricci curvature R is given by $R = -n(n-1)K$.

4.2 n -component reactive temporal neurodynamics

If we drop the diffusion term in the general reaction–diffusion equation (1), we get a purely reactive temporal dynamics, reducing a single n D parabolic PDE to an n D system of nonlinear ODEs. In this subsection we will explore nonlinear temporal dynamics of (Hopfield–type) neural networks.

4.2.1 Neurons as functions

It is a common view in computational intelligence that neurons behave as functions (see [44, 30, 35]): they transduce an unbounded input *activation* $x(t)$ into output *signal* $S(x(t))$. Usually a sigmoidal (S-shaped, bounded, monotone-nondecreasing: $S' \geq 0$) function describes the transduction, as well as the input–output behavior of many operational amplifiers. For example, the *logistic signal* (or, the *maximum–entropy*) function

$$S(x) = \frac{1}{1 + e^{-cx}}$$

is sigmoidal and strictly increases for positive scaling constant $c > 0$. Strict monotonicity implies that the *activation derivative* of S is positive:

$$S' = \frac{dS}{dx} = cS(1 - S) > 0.$$

Another frequent bipolar signal function is the *hyperbolic–tangent*,

$$S(x) = \tanh(cx) = \frac{e^{cx} - e^{-cx}}{e^{cx} + e^{-cx}},$$

with activation derivative

$$S' = c(1 - S^2) > 0.$$

Also, the *Gaussian*, or bell-shaped, signal function of the form $S(x) = e^{-cx^2}$, for $c > 0$, represents an important exception to signal monotonicity. Its activation derivative $S' = -2cxe^{-cx^2}$ has the sign opposite the sign of the activation x .

The *signal velocity* $\dot{S} \equiv dS/dt$ is the *signal time derivative*, related to the activation derivative by

$$\dot{S} = S'\dot{x},$$

so it depends explicitly on *activation velocity*. This is used in unsupervised learning laws that adapt with *locally available information*.

The signal $S(x)$ induced by the activation x represents the neuron’s firing frequency of action potentials, or pulses, in a sampling interval. The firing frequency equals the average number of pulses emitted in a sampling interval.

Short-term memory is modelled by *activation dynamics*, and *long-term memory* is modelled by *learning dynamics*. The overall neural network behaves as an *adaptive filter* (see [22]).

Continuous ANNs are *temporal dynamical systems* with two coupled dynamics: activation and learning. First, a general system of coupled ODEs for the output of the i th *processing element* (PE) x^i , called the *activation dynamics*, can be written as

$$\dot{x}^i = g_i(x^i, \text{net}_i), \quad (55)$$

with the *net input* to the i th PE x^i given by $\text{net}_i = \omega_{ij}x^j$.

For example,

$$\dot{x}^i = -x^i + f_i(\text{net}_i),$$

where f_i is called *output*, or *activation*, *function*. We apply some input values to the PE so that $\text{net}_i > 0$. If the inputs remain for a sufficiently long time, the output value will reach an equilibrium value, when $\dot{x}^i = 0$, given by $x^i = f_i(\text{net}_i)$. Once the unit has a nonzero output value, removal of the inputs will cause the output to return to zero. If $\text{net}_i = 0$, then $\dot{x}^i = -x^i$, which means that $x \rightarrow 0$.

Second, a general system of coupled ODEs for the *update* of the synaptic weights ω_{ij} , i.e. *learning dynamics*, can be written as a generalization of the Oja–Hebb rule, i.e..

$$\dot{\omega}_{ij} = G_i(\omega_{ij}, x^i, x^j),$$

where G_i represents the *learning law*; the learning process consists of finding weights that encode the knowledge that we want the system to learn. For most realistic systems, it is not easy to determine a closed-form solution for this system of equations, so the approximative solutions are usually enough.

4.2.2 Activation dynamics

Hopfield’s graded–response neurons²¹ have continuous input–output relation (like nonlinear operational amplifiers) of the form $V_i = g_i(\lambda u_i)$, where u_i denotes the input at i , a

²¹The paradigm for the unsupervised, self–organizing, associative, and recurrent ANN is the discrete Hopfield network (see [24]). Hopfield gives a collection of simple threshold automata, called *formal neurons* by McCulloch and Pitts (see [30, 35]): two–state, ‘all–or–none’, firing or non–firing units that can be modelled by *Ising spins* (uniaxial magnets) $\{S_i\}$ such that $S_i = \pm 1$ (where $1 = |\uparrow\rangle =$ ‘spin up’ and $-1 = |\downarrow\rangle =$ ‘spin down’; the label of the neuron is i and ranges between 1 and the size of the network N). The neurons are connected by synapses J_{ij} .

Firing *patterns* $\{\xi_i^\mu\}$ represent specific S_i –*spin configurations*, where the label of the pattern is μ and ranges between 1 and q . Using random patterns $\xi_i^\mu = \pm 1$ with equal probability 1/2, we have the *synaptic efficacy* J_{ij} of j th neuron operating on i th neuron given by

$$J_{ij} = N^{-1} \xi_i^\mu \xi_j^\mu \equiv N^{-1} \xi_i \cdot \xi_j. \quad (56)$$

constant λ is called the gain parameter, and V_i is the output [25]. Usually, g_i are taken to be sigmoid functions, odd, and monotonically increasing (e.g., $g(\cdot) = \frac{1}{2}(1 + \tanh(\cdot))$), while discrete Ising spins have $g_i(u_i) = \text{sgn}_i(u_i)$. The behavior of the *continuous Hopfield network* is usually described by a set of coupled RC-transient equations

$$C_i \dot{u}_i = I_i + J_{ij} V_j - \frac{u_i}{R_i}, \quad (60)$$

where $u_i = g^{-1}(V_i)$, R_i and C_i denote input capacitance and resistance, and I_i represents an external source.

Using random patterns $\xi_i^\mu = \pm 1$ with equal probability 1/2, we have the *synaptic efficacy* J_{ij} of j th neuron operating on i th neuron given by²²

$$J_{ij} = N^{-1} \xi_i^\mu \xi_j^\mu \equiv N^{-1} \boldsymbol{\xi}_i \cdot \boldsymbol{\xi}_j. \quad (61)$$

The Hamiltonian of the continuous system (60) is given by

$$H = -\frac{1}{2} J_{ij} V_i V_j + \sum_{i=1}^N R_i^{-1} \int_0^{V_i} dV g^{-1}(V) - I_i V_i. \quad (62)$$

However, according to Hopfield [25] the synapses J_{ij} retain the form (61) with random patterns $\xi_i^\mu = \pm 1$ with equal probability 1/2, and the synaptic symmetry $J_{ij} = J_{ji}$ implies

Postsynaptic potential (PSP) represents an *internal local field*

$$h_i(t) = J_{ij} S_j(t). \quad (57)$$

Now, the *sequential (threshold) dynamics* is defined in the form of discrete equation

$$S_i(t + \Delta t) = \text{sgn}[h_i(t)]. \quad (58)$$

Dynamics (58) is equivalent to the rule that the state of a neuron is changed, or a spin is flipped iff the total network *energy*, given by *Ising Hamiltonian*

$$H_N = -\frac{1}{2} J_{ij} S_i S_j, \quad (59)$$

is lowered [24]. Therefore, the Ising Hamiltonian H_N represents the monotonically decreasing *Lyapunov function* for the sequential dynamics (58), which converges to a local minimum or ground state of H_N . This holds for any *symmetric coupling* $J_{ij} = J_{ji}$ with $J_{ii} = 0$ and if spin-updating in (58) is asynchronous. In this case the patterns $\{\xi_i^\mu\}$ after convergence become identical, or very near to, ground states of H_N , each of them at the bottom of the valley.

²²More general form of synapses is

$$J_{ij} = N^{-1} Q(\boldsymbol{\xi}_i; \boldsymbol{\xi}_j),$$

for some synaptic kernel Q on $\mathbb{R}^n \times \mathbb{R}^n$. The vector $\boldsymbol{\xi}_i$ varies as i travels from 1 to N , but remains on a corner of the *Hamming hypercube* $[-1, 1]^n$.

that the continuous Hamiltonian (62) represents a *Lyapunov function* of the system (60), i.e., H decreases under the continual neuro-dynamics governed by equation (60) as time proceeds.

4.2.3 Hopfield's overlaps

Assuming that the number q of stored patterns is small compared to the number of neurons, i.e., $q/N \rightarrow 0$, we find that the synapses (61) give rise to a local field of the form

$$h_i = \xi_i^\mu m_\mu, \quad \text{where} \quad (63)$$

$$m_\mu = N^{-1} \xi_i^\mu S_i \quad (64)$$

is the *auto-overlap* (or simply *overlap*)²³ of the network state $\{S_i\}$ with the pattern $\{\xi_i^\mu\}$, measuring the proximity between them. We can see that $m_\mu = 1$ (like peak-up in auto-correlation) if $\{S_i\}$ and $\{\xi_i^\mu\}$ are identical patterns, $m_\mu = -1$ (like peak-down in autocorrelation) if they are each other's complement, and $m_\mu = O(1/\sqrt{N})$ if they are uncorrelated (like no-peak in auto-correlation) with each other. Overlaps m_μ are related to the Hamming distance d_μ between the patterns (the fraction of spins which differ) by $d_\mu = \frac{1}{2}(1 - m_\mu)$.

As a pattern ξ_i^μ represents (in the simplest case) a specific Ising-spin S_i -configuration, then $(\xi_i^\mu)^2 = 1$. If $S_i = \xi_i^\mu$ for all i , then $m_\mu = 1$. Conversely, if $m_\mu = 1$, then $S_i = \xi_i^\mu$. In all other cases $m_\mu < 1$, by the Cauchy-Schwartz inequality. If ξ_i^μ and S_i are uncorrelated, we may expect m_μ to be of the order of $N^{-1/2}$, since the sum consists of N terms, each containing a ξ_i^μ . On the other hand, if the S_i are positively correlated with ξ_i^μ , then m_μ is of the order of unity. So the overlaps give the global information about the network and hence are good order parameters. Also, according to Hopfield [25], the extension to the continual network is straightforward.

Using overlaps, the *Ising Hamiltonian* becomes

$$H_N = -\frac{1}{2}N \sum_{\mu=1}^q m_\mu^2. \quad (65)$$

The similarity between two different patterns ξ_i^μ and ξ_i^ν is measured by their *mutual overlap* or *cross-overlap* $m_{\mu\nu}$ (in other parlance it is called *Karhunen-Loeve covariance matrix* (see [35]), which extracts the principal components from a data set)²⁴, equal

$$m_{\mu\nu} = N^{-1} \xi_i^\mu \xi_i^\nu. \quad (66)$$

²³resembling the auto-correlation function of a time-series, where distinct peaks indicate that the series at the certain time t is similar to the series at time $t + \Delta t$

²⁴resembling the cross-correlation function of two time-series, with several distinct peaks, indicating that the two series are very similar at each point in time where the peaks occur

For similar patterns the cross-overlap is close to unity whereas for uncorrelated patterns it is random variable with zero mean and small $(1/\sqrt{N})$ variance.

The symmetric *Hopfield synaptic matrix* J_{ij} can be expressed in terms of the cross-overlaps $m_{\mu\nu}$ as

$$J_{ij} = N^{-1} \xi_i^\mu (m_{\mu\nu})^{-1} \xi_j^\nu = J_{ji}, \quad (67)$$

where $(m_{\mu\nu})^{-1}$ denotes the *Moore–Penrose pseudoinverse* of the cross-overlap matrix $m_{\mu\nu}$.

Besides the Hopfield model, the proposed pattern-overlap picture can be extended to cover some more sophisticated kinds of associative memory, among them [35]:

1. Forgetful memories, characterized by iterative synaptic prescription

$$J_{ij}^{(\mu)} = \phi(\epsilon \xi_i^\mu \xi_j^\mu + J_{ij}^{(\mu-1)}),$$

for some small parameter ϵ and some odd function ϕ . If $\phi(\cdot)$ saturates as $|\cdot| \rightarrow \infty$, the memory creates storage capacity for new patterns by forgetting the old ones.

2. Temporal associative memories, which can store and retrieve a sequence of patterns, through synapses

$$N J_{ij} = \xi_i^\mu \xi_j^\mu + \epsilon \sum_{\mu=1}^q \xi_i^{(\mu+1)} \xi_j^\mu, \quad (68)$$

where the second term on the right is associated with a temporal delay, so that one can imagine that the second term ‘pushes’ the neural system through an energy landscape created by the first term.

4.2.4 Glauber vs. overlap dynamics

According to Hopfield [25], the extension of the sequential dynamics $S_i = \text{sgn}(\sum_{\mu} m_{\mu} \xi_i^{\mu})$ of the network made of the simplest Ising-spin-neurons to the network made of continuous graded-response amplifier-neurons, is straightforward using the probabilistic *Glauber dynamics*

$$\text{Prob}\{S_i \mapsto -S_i\} = \frac{1}{2}[1 - \tanh(\beta h_i S_i)], \quad (i = 1, \dots, N), \quad (69)$$

where β represents the universal temperature ($\beta = \frac{1}{k_B T}$, k_B is the normalized Boltzman’s constant and $k_B T$ has dimension of energy).

Under the Glauber’s dynamics (69), and as $N \rightarrow \infty$ (transition from the single neurons to the neural field), for time-dependent patterns $\xi^\mu(t) = \xi_\mu(t)$, vector auto-overlaps $m_\mu(t)$, and tensor cross-overlaps $m_{\mu\nu}(t)$, we present the dynamics of overlaps governed by the following nonlinear differential equations [35]

$$\dot{m}_\mu(t) = -m_\mu(t) + \langle \xi_\mu(t) \tanh[\beta m_\mu(t) \xi^\mu(t)] \rangle, \quad (70)$$

and in the tensor form

$$\dot{m}_{\mu\nu}(t) = -m_{\mu\nu}(t) + \langle \xi_\mu(t)\xi_\nu(t) \tanh[\beta m_{\mu\nu}(t)\xi^\mu(t)\xi^\nu(t)] \rangle, \quad (71)$$

where the angular brackets denote an average over the q patterns $\xi^\mu(t)$.

The stationary solutions (for any fixed instant of time $t = \tau$) of equations (70) and (71) are given by corresponding fixed–point vector and tensor equations

$$m_\mu = \langle \xi_\mu \tanh[\beta m_\mu \xi^\mu] \rangle, \quad \text{and} \quad (72)$$

$$m_{\mu\nu} = \langle \xi_\mu \xi_\nu \tanh[\beta m_{\mu\nu} \xi^\mu \xi^\nu] \rangle, \quad (73)$$

respectively.

4.2.5 Generalized Hebbian learning dynamics

In terms of stochastic feed–forward multi–layer neural networks, the tensorial equation (71) corresponds to the average, general, self–organizing Hebbian neural learning scheme (see [23, 44])

$$\dot{m}_{\mu\nu}(t) = -m_{\mu\nu}(t) + \langle \mathcal{I}_{\mu\nu} \rangle, \quad (74)$$

with random signal *Hebbian innovation*

$$\mathcal{I}_{\mu\nu} = f_\mu[\xi^\mu(t)] f_\nu[\xi^\nu(t)] + \sigma_{\mu\nu}(t), \quad (75)$$

where $\sigma_{\mu\nu}$, denotes the tensorial, additive, zero–mean, Gaussian white–noise, independent of the main innovation function $I_{\mu\nu}$, while $f_{\mu,\nu}[\cdot]$ represent the hyperbolic tangent (sigmoid) neural activation functions. A single–layer Hebbian learning scheme, corresponding to the tensor equation (74), gives

$$\dot{m}_\mu(t) = -m_\mu(t) + \langle \mathcal{I}_\mu \rangle, \quad (76)$$

with the vector innovation

$$\mathcal{I}_\mu = f_\mu[\xi^\mu(t)] + \sigma_\mu(t),$$

where σ_μ , denotes the vector additive zero–mean Gaussian white–noise, also independent of the main innovation function I_μ , while $f_\mu[\cdot]$ represents the hyperbolic tangent (sigmoid) neural activation function.

If we assume the small absolute value of the average (stochastic) terms, the nonlinear overlap–dynamics equations (70) and (71) can be presented in the form of *weakly–connected neural networks* (see [26]), respectively, as a single–layer network

$$\dot{m}_\mu(t) = -m_\mu(t) + \varepsilon g_\mu(m_\mu, \varepsilon), \quad \varepsilon \ll 1, \quad (77)$$

and a multi–layer network

$$\dot{m}_{\mu\nu}(t) = -m_{\mu\nu}(t) + \varepsilon g_{\mu\nu}(m_{\mu\nu}, \varepsilon), \quad \varepsilon \ll 1, \quad (78)$$

where, g_μ and $g_{\mu\nu}$, corresponding to the average (bracket) terms in (70) and (71), describe (vector and tensor, respectively) synaptic connections and the ‘small’ parameter ε describes their (dimensionless) strength. These weakly-connected neural systems represent ε -perturbations of the corresponding linear systems

$$\dot{m}_\mu(t) = -m_\mu(t) \quad \text{and} \quad \dot{m}_{\mu\nu}(t) = -m_{\mu\nu}(t),$$

with exponential maps as solutions

$$m_\mu(t) = m_\mu e^{-t} \quad \text{and} \quad m_{\mu\nu}(t) = m_{\mu\nu} e^{-t},$$

using the stationary (fixed-point) solutions (72, 73) as initial conditions m_μ and $m_{\mu\nu}$. According to the *Hartman–Grobman theorem* from dynamical systems theory, the weakly-connected systems (77, 78) are topologically equivalent (homeomorphic) to the corresponding linear systems. Therefore the whole analysis for the linear vector and matrix flows can be applied here, with only difference that instead of increasing transients e^t here we have decreasing (i.e., asymptotically-stable) transients e^{-t} .

On the other hand, in terms of *synergetics* [21], both nonlinear overlap-dynamics equations (70–71) and Hebbian learning equations (74–75), represent (covariant) *order parameter equations*.

By introducing the scalar quadratic potential fields, dependent on vector and tensor order parameters (overlaps), respectively

$$V(m_\mu) = -\frac{1}{2} \sum_{\mu=1}^q m_\mu^2 \quad \text{and} \quad V(m_{\mu\nu}) = -\frac{1}{2} m_{\mu\nu}^2,$$

we can generalize the overlap-dynamics equations (70–71) to the *stochastic-gradient order parameter equations*, in vector and tensor form, respectively

$$\dot{m}_\mu(t) = -\frac{\partial V(m_\mu)}{\partial m_\mu(t)} + F_\mu(t), \quad \text{and} \quad (79)$$

$$\dot{m}_{\mu\nu}(t) = -\frac{\partial V(m_{\mu\nu})}{\partial m_{\mu\nu}(t)} + F_{\mu\nu}(t). \quad (80)$$

$F_\mu(t)$ in (79) represents a vector fluctuating force, with average (over the stochastic process which produces the fluctuating force $F_\mu(t)$)

$$\langle F_\mu(t) \rangle = \langle \xi_\mu(t) \tanh[\beta m_\mu(t) \xi^\mu(t)] \rangle,$$

and variation

$$\langle F_\mu(t) F_\mu(t') \rangle = Q_\mu \delta(t - t'), \quad (81)$$

while $F_{\mu\nu}(t)$ in (80) represents a tensor fluctuating force, with average (over the stochastic process which produces the fluctuating force $F_{\mu\nu}(t)$)

$$\langle F_{\mu\nu}(t) \rangle = \langle \xi_\mu(t) \xi_\nu(t) \tanh[\beta m_{\mu\nu}(t) \xi^\mu(t) \xi^\nu(t)] \rangle,$$

and variation

$$\langle F_{\mu\nu}(t) F_{\mu\nu}(t') \rangle = Q_{\mu\nu} \delta(t - t'). \quad (82)$$

Coefficients Q_μ in (81) and $Q_{\mu\nu}$ in (82) represent strengths of the corresponding stochastic processes, while Dirac δ -functions $\delta(t - t')$ express their short-term memories.

Recall that standard interpretation of synergetics (see [21]) describes the stochastic gradient systems (79–80) as the overdamped motion of (vector and tensor, respectively) representative particles in scalar potential fields $V(m_\mu)$ and $V(m_{\mu\nu})$, subject to fluctuating forces $F_\mu(t)$ and $F_{\mu\nu}(t)$. These particles undergo *non-equilibrium phase transitions* (in the similar way as the magnet undergoes transition from its unmagnetized state into a magnetized state, or a superconductor goes from its normal state into the superconducting state, only occurring now in systems far from thermal equilibrium), and associated phenomena, including a *symmetry breaking instability* and *critical slowing down* (see [21]).

The non-equilibrium phase transitions of vector and tensor order parameters (overlaps) $m_\mu(t)$ and $m_{\mu\nu}(t)$, are in synergetics described in terms of probability distributions $p(m_\mu, t)$ and $p(m_{\mu\nu}, t)$, respectively, defined by corresponding *Fokker-Planck equations*

$$\begin{aligned} \dot{p}(m_\mu, t) &= p(m_\mu, t) + \frac{1}{2} Q_\mu \frac{\partial^2 p(m_\mu, t)}{\partial m_\mu^2}, \quad \text{and} \\ \dot{p}(m_{\mu\nu}, t) &= p(m_{\mu\nu}, t) + \frac{1}{2} Q_{\mu\nu} \frac{\partial^2 p(m_{\mu\nu}, t)}{\partial m_{\mu\nu}^2}. \end{aligned}$$

4.2.6 Lotka–Volterra–based associative net

Hopfield recurrent associative memory network can be generalized to get a *bidirectional associative memory* network, the so-called BAM model of Kosko [44]. Here we derive an alternative self-organizing neural net model with competitive *Lotka-Volterra ensemble dynamics*²⁵ (see [70, 30]).

²⁵The competitive Lotka-Volterra equations are a simple model of the population dynamics of two species competing for some common resource. It is the pair of coupled logistic ODEs for two competing populations with sizes x_1, x_2 ,

$$\dot{x}_1 = r_1 x_1 \left(\frac{K_1 - x_1 - \alpha_{12} x_2}{K_1} \right) \quad (83)$$

$$\dot{x}_2 = r_2 x_2 \left(\frac{K_2 - x_2 - \alpha_{21} x_1}{K_2} \right), \quad (84)$$

where $r_{1,2}$ are their growth rates, $K_{1,2}$ are their respective carrying capacities, while $\alpha_{1,2}, \alpha_{2,1}$ are the mutual (coupling) effects of one species onto another.

We start from $(n + m)$ D linear ODEs, describing two competitive neural ensembles participating in a two-party game,

$$\begin{aligned}\dot{R}^i &= -\alpha_B^j B_j, & R^i(0) &= R_0^i, \\ \dot{B}_j &= -\beta_i^R R^i, & B_j(0) &= B_j^0, \end{aligned} \quad (i = 1, \dots, n; j = 1, \dots, m), \quad (85)$$

where $R^i = R^i(t)$ and $B_j = B_j(t)$ respectively represent the numerical strengths of the two neural ensembles at time t , R_0^i, B_j^0 are their initial conditions, and α_B and β^R represent the effective spiking rates (which are either constant, or Poisson random process). In this way, we generate a $(n + m)$ D smooth manifold M , a *neural state-space*, and two dynamical objects acting on it: an n D smooth *vector-field* \dot{R}^i , and an m D differential 1-form \dot{B}_j . Their dot product $\dot{R}^i \cdot \dot{B}_j$, represents a hypothetical *neural outcome*. This is a linear system, with the passive-decay couplings $\alpha_B^j B_j$ and $\beta_i^R R^i$, fully predictable but giving only equilibrium solutions.

Secondly, to incorporate competitive dynamics of Volterra-Lotka style as commonly used in ecological modelling and known to produce a global chaotic attractor [32], we include to each of the neural ensembles a nonlinear competing term depending only on its own units,

$$\begin{aligned}\dot{R}^i &= a^i R^i(1 - b^i R^i) - \alpha_B^j B_j, \\ \dot{B}_j &= c_j B_j(1 - d_j B_j) - \beta_i^R R^i. \end{aligned} \quad (86)$$

Now we have a *competition between the two chaotic attractors*, one for the R^i and one for the B_j ensemble, i.e., the two self-organization patterns emerging far-from-equilibrium.

Thirdly, to make this even more realistic, we include the ever-present *noise* in the form of Langevin-type random forces $F^i = F^i(t)$, and $G_j = G_j(t)$, thus adding the ‘neural heating’, i.e., noise induced entropy growth, to the competitive dynamics

$$\begin{aligned}\dot{R}^i &= a^i R^i(1 - b^i R^i) - \alpha_B^j B_j + F^i, \\ \dot{B}_j &= c_j B_j(1 - d_j B_j) - \beta_i^R R^i + G_j. \end{aligned} \quad (87)$$

Finally, to overcome the deterministic chaos and stochastic noise with an adaptive *brain-like dynamics*, we introduce the *field competition potential* V , in the scalar form

$$V = -\frac{1}{2}(\omega_i^j R^i B_j + \varepsilon_i^j B_j R^i), \quad (88)$$

where ω_i^j and ε_i^j represent *synaptic associative-memory* matrices for the R^i and B_j ensemble, respectively. From the negative potential V , we get a *Lyapunov-stable gradient system* $\dot{R}^i = -\frac{\partial V}{\partial B_j}$, $\dot{B}_j = -\frac{\partial V}{\partial R^i}$. This robust system, together with the *sigmoidal activation functions* $S(\cdot) = \tanh(\cdot)$, and *control inputs* $u_{OLN}^i = u_{OLN}^i(t)$ and $v_j^{OLN} = v_j^{OLN}(t)$,

we incorporate into (87) to get the *full neural competitive–associative dynamics*

$$\begin{aligned}
\dot{R}^i &= u_{OLN}^i - \alpha_B^j B_j + a^i R^i (1 - b^i R^i) + \omega_i^j S_j(B_j) + F^i, \\
\dot{B}_j &= v_j^{OLN} - \beta_i^R R^i + c_j B_j (1 - d_j B_j) + \varepsilon_i^j S^i(R^i) + G_j, \\
&\text{with initial conditions} \\
R^i(0) &= R_0^i, \quad B_j(0) = B_j^0.
\end{aligned} \tag{89}$$

Now, each ensemble learns by trial–and–error from the opposite side. In a standard ANN–fashion, we model this learning on the spot by initially setting the random values to the synaptic matrices ω_i^j and ε_i^j , and subsequently adjust these values using the standard *Hebbian learning scheme* [23]:

$$\text{New Value} = \text{Old Value} + \text{Innovation},$$

which in our case reads:

$$\begin{aligned}
\dot{\omega}_i^j &= -\omega_i^j + \Phi_i^j(R^i, B_j), \\
\dot{\varepsilon}_i^j &= -\varepsilon_i^j + \Psi_i^j(B_j, R^i),
\end{aligned} \tag{90}$$

with *innovation* given in tensor signal form (generalized from [44])

$$\begin{aligned}
\Phi_i^j &= S_j(R^i) S_j(B_j) + \dot{S}_j(R^i) \dot{S}_j(B_j), \\
\Psi_i^j &= S^i(R^i) S^i(B_j) + \dot{S}^i(R^i) \dot{S}^i(B_j),
\end{aligned} \tag{91}$$

where terms with overdots, equal $\dot{S}(\cdot) = 1 - \tanh(\cdot)$, denote the *signal velocities*.

References

- [1] M.J. ABLOWITZ, D.J. KAUP, A.C. NEWELL, AND H. SEGUR, Method for solving the sine-Gordon equation. Phys. Rev. Let. 30(1973), pp. 1262–1264.
- [2] N.N. AKHMEDIEV, V.M. ELEONSKII, AND N.E. KULAGIN, First-order exact solutions of the nonlinear Schrödinger equation. Th. Math. Physics 72(1987), pp. 809–818.
- [3] S. AMARI, Dynamics of pattern formation in lateral-inhibition type neural fields. Biol. Cybern. 27(1977), pp. 77–87.
- [4] M.T. ANDERSON, Geometrization of 3-manifolds via the Ricci flow, Not. Am. Math. Soc. 512(2004), pp. 184–193.
- [5] D. BARKLEY, A model for fast computer–simulation of waves in excitable media. Physica D 49(1991), pp. 61–70.

- [6] M. BODE, Front-bifurcations in reaction-diffusion systems with inhomogeneous parameter distributions, *Physica D* 106(1997), pp. 270–286.
- [7] H.D. CAO AND B. CHOW, Recent developments on the Ricci flow, *Bull. Amer. Math. Soc.* 36(1999), pp. 59-74.
- [8] B. CHOW AND D. KNOPF, *The Ricci flow: An introduction*, Mathematical Surveys and Monographs, AMS, Providence, RI, (2004).
- [9] J.M. CONWAY AND H. RIECKE, Superlattice Patterns in the Complex Ginzburg-Landau Equation with Multi-Resonant Forcing, arXiv:nlin.PS.0803.0346, (2008).
- [10] R.J. FIELD, Oregonator, *Scholarpedia*, 2:5(2007), pp. 1386.
- [11] R.J. FIELD, E. KOLOSOS, AND R.M. NOYES, Oscillations in chemical systems. *J. Amer. Chem. Soc.* 94(1972), pp. 8649–8664.
- [12] R. FITZHUGH, Impulses and physiological states in theoretical models of nerve membrane. *Biophys. J.* 1(1961), pp. 445-466.
- [13] R. FRIEDRICH, *Group Theoretic Methods in the Theory of Pattern Formation*, in *Collective dynamics of nonlinear and disordered systems*, Springer, Berlin, (2004).
- [14] A. GIERER AND H. MEINHARDT, A theory of biological pattern formation. *Kybernetik* 12(1972), pp. 30-39.
- [15] S.V. GUREVICH, S. AMIRANASHVILI, AND H.-G. PURWINS, Breathing dissipative solitons in three-component reaction-diffusion system. *Phys. Rev. E* 74(2006), pp. 066201.
- [16] R.S. HAMILTON, Three-manifolds with positive Ricci curvature, *J. Diff. Geom.* 17(1982), pp. 255-306.
- [17] R.S. HAMILTON, Four-manifolds with positive curvature operator, *J. Dif. Geom.* 24(1986), pp. 153-179.
- [18] R.S. HAMILTON, The Ricci flow on surfaces, *Cont. Math.* 71(1988), pp. 237-261.
- [19] R.S. HAMILTON, The Harnack estimate for the Ricci flow, *J. Dif. Geom.* 37(1993), pp. 225-243.
- [20] R.S. HAMILTON, Non-singular solutions of the Ricci flow on three-manifolds, *Comm. Anal. Geom.*, 7:4(1999), pp. 695-729.
- [21] H. HAKEN, *Synergetics: An Introduction* (3rd ed). Springer, Berlin, (1983)

- [22] S. HAYKIN, Adaptive Filter Theory. Prentice–Hall, Englewood Cliffs, (1991)
- [23] D.O. HEBB, The Organization of Behavior, Wiley, New York, (1949)
- [24] J.J. HOPFIELD, Neural networks and physical systems with emergent collective computational abilities. Proc. Natl. Acad. Sci. USA **79**, 2554, (1982)
- [25] J.J. HOPFIELD, Neurons with graded response have collective computational properties like those of two–state neurons. Proc. Natl. Acad. Sci. USA, **81**, 3088–3092, (1984)
- [26] F.C. HOPPENSTEADT AND E.M. IZHIKEVICH, Weakly Connected Neural Networks. Springer, New York, (1997)
- [27] S. HAWKING AND R. PENROSE, The Nature of Space and Time, Princeton Univ. Press, (1996).
- [28] S.Y. HSU, Some results for the Perelman LYH-type inequality, arXiv:math.DG/0801.3506, (2008).
- [29] V. IVANCEVIC, Symplectic Rotational Geometry in Human Biomechanics, SIAM Rev. 46:3(2004), pp. 455–474.
- [30] IVANCEVIC, V. AND IVANCEVIC, T., Natural Biodynamics. World Scientific, Singapore, (2006).
- [31] V. IVANCEVIC AND T. IVANCEVIC, Geometrical Dynamics of Complex Systems. Springer, Dordrecht, (2006).
- [32] V. IVANCEVIC AND T. IVANCEVIC, High–Dimensional Chaotic and Attractor Systems. Springer, Berlin, (2006).
- [33] V. IVANCEVIC AND T. IVANCEVIC, Complex Dynamics: Advanced System Dynamics in Complex Variables. Springer, Dordrecht, (2007).
- [34] V. IVANCEVIC AND T. IVANCEVIC, Applied Differential Geometry: A Modern Introduction. World Scientific, Singapore, (2007).
- [35] V. IVANCEVIC AND T. IVANCEVIC, Neuro-Fuzzy Associative Machinery for Comprehensive Brain and Cognition Modelling. Springer, Berlin, (2007).
- [36] V. IVANCEVIC AND T. IVANCEVIC, Computational Mind: A Complex Dynamics Perspective. Springer, Berlin, (2007).
- [37] V. IVANCEVIC AND T. IVANCEVIC, Complex Nonlinearity: Chaos, Phase Transitions, Topology Change and Path Integrals. Springer, Berlin, (2008).

- [38] V. IVANCEVIC AND T. IVANCEVIC, Quantum Leap: From Dirac and Feynman, Across the Universe, to Human Body and Mind. World Scientific, Singapore, (2008).
- [39] T. IVANCEVIC, L. JAIN, J. PATTISON, AND A. HARIZ, Nonlinear Dynamics and Chaos Methods in Neurodynamics and Complex Data Analysis. *Nonl. Dyn.* (to appear, On line first, Springer).
- [40] A. KAMINAGA, V.K. VANAG, AND I.R. EPSTEIN, “Black spots” in a surfactant-rich Belousov-Zhabotinsky reaction dispersed in a water-in-oil microemulsion system. *J. Chem. Phys.* 122(2005), pp. 174706.
- [41] A. KAMINAGA, V.K. VANAG, AND I.R. EPSTEIN, A reaction-diffusion memory device. *Ang. Chem.* 45(2006), pp. 3087.
- [42] G. KOHLER AND C. MILSTEIN, Continuous cultures of fused cells secreting antibody of predefined specificity. *Nature*, 256(1975), pp. 495.
- [43] T. KOLOKOLNIKOV AND M. TLIDI, Spot deformation and replication in the two-dimensional Belousov-Zhabotinsky reaction in water-in-oil microemulsion, *Phys. Rev. Lett.* 98(2007), pp. 188303.
- [44] B. KOSKO, Neural Networks and Fuzzy Systems, A Dynamical Systems Approach to Machine Intelligence. Prentice–Hall, New York, (1992)
- [45] L.A. KUNZ-SCHUGHART, Multicellular tumor spheroids: intermediates between monolayer culture and in vivo tumor, *Cell Biol. Int.* 23:3(1999), pp. 157-61.
- [46] P. LI AND S.T. YAU, On the parabolic kernel of the Schrödinger operator. *Acta Math.* 156(1986), pp. 153–201.
- [47] J. LI, First variation of the Log Entropy functional along the Ricci flow, [arXiv:math.DG/0712.0832](https://arxiv.org/abs/math/0712.0832), (2007).
- [48] D. MACKENZIE, Perelman Declines Math’s Top Prize; Three Others Honored in Madrid, *Science* 313, pp. 1027, (2006).
- [49] H. MEINHARDT, Gierer-Meinhardt model, *Scholarpedia*, 1:12(2006), pp. 1418.
- [50] J. MILNOR, Towards the Poincaré Conjecture and the Classification of 3-Manifolds, *Not. Am. Math. Soc.* 50:10(2003), pp. 1226-1233.
- [51] C. MISNER, K. THORNE, AND J.A. WHEELER, Gravitation, W.H. Freeman and Company, (1973).

- [52] A.R. MISSEL AND K.A. DAHMEN, Hopping Conduction and Bacteria: Transport in Disordered Reaction-Diffusion Systems, *Phys. Rev. Let.* 100(2007), pp. 058301.
- [53] S.W. MORGAN, I.V. BIKTASHEVA, AND V.N. BIKTASHEV, Control of scroll wave turbulence using resonant perturbations. *arXiv:nlinPS.0806.2262*, (2008).
- [54] J. NAGUMO, S. ARIMOTO, S. YOSHIKAWA, An active pulse transmission line simulating nerve axon. *Proc IRE.* 50(1962), pp. 2061–2070.
- [55] D.R. NELSON AND N.M. SHNERB, Non-hermitian localization and population biology. *Phys. Rev. E* 58(1998), pp. 1383–1403.
- [56] K. NIELSEN, F. HYNNE, P.G. SORENSEN, Hopf bifurcation in chemical kinetics, *J. Chem. Phys.* textbf94(1991), pp. 1020–1029.
- [57] R. PENROSE, Singularities and Time-Asymmetry, in *General Relativity: An Einstein Centenary Survey*, (ed. S. Hawking, W. Israel), 581–638, Cambridge Univ. Press, (1979).
- [58] G. PERELMAN, The entropy formula for the Ricci flow and its geometric applications, *arXiv:math.DG/0211159*, (2002).
- [59] G. PERELMAN, Ricci flow with surgery on three-manifolds, *arXiv:math.DG/0303109*, (2003).
- [60] L. PREZIOSI, *Cancer Modeling and Simulation*. CRC Press, (2003).
- [61] I. PRIGOGINE, *From Being to Becoming: Time and Complexity in the Physical Sciences*. Freeman, San Francisco, (1980).
- [62] H.-G. PURWINS, H.U. BODEKER, AND A.W. LIEHR, Dissipative Solitons in Reaction-Diffusion Systems, in *Dissipative Solitons* (ed. N. Akhmediev, A. Ankiewicz), *Lecture Notes in Physics*, Springer, (2005).
- [63] M.I. RABINOVICH, A.B. EZERSKY, AND P.D. WEIDMAN, *The Dynamics of Patterns*, World Scientific, Singapore, (2000).
- [64] T. ROOSE, S.J. CHAPMAN, P.K. MAINI, Mathematical Models of Avascular Tumor Growth. *SIAM Rev.* 49:2(2007), pp. 179–208.
- [65] G. SCHÖNER, *Dynamical Systems Approaches to Cognition*. In: *Cambridge Handbook of Computational Cognitive Modeling*. Cambridge University Press. R. Sun (ed), (2007).

- [66] R.M. SUTHERLAND, Cell and environment interactions in tumor microregions: The multicell spheroid model, *Science*, 240(1988), pp. 177–184.
- [67] W. THURSTON, Three-dimensional manifolds, Kleinian groups and hyperbolic geometry, *Bull. Amer. Math. Soc.* 6(1982), pp. 357-381.
- [68] A.M. TURING, The Chemical Basis of Morphogenesis. *Phil. Trans. Roy. Soc. London*, B 237(1952), pp. 37–72.
- [69] J.J. TYSON, A quantitative account of oscillations, bistability and travelling waves in the Belousov-Zhabotinskii reaction, in *Oscillation and Travelling Waves in Chemical Systems*, eds. Field, R. J., Burger, M., Wiley-Intersc., New York, (1985).
- [70] V. VOLTERRA, Variations and fluctuations of the number of individuals in animal species living together, in *Animal Ecology*. McGraw-Hill, (1931).
- [71] S.T. YAU, Structure of Three-Manifolds — Poincaré and geometrization conjectures. talk given at the Morningside Center of Mathematics on June 20, (2006).
- [72] R. YE, The log entropy functional along the Ricci flow. *arXiv:math.DG/0708.2008v3*, (2007).
- [73] A.M. ZHABOTINSKY, Belousov–Zhabotinsky reaction, *Scholarpedia*, 2:9(2007), pp. 1435.